



Article

Zygo-Albuside A: New Saponin from *Zygophyllum album* L. with Significant Antioxidant, Anti-Inflammatory and Antiapoptotic Effects against Methotrexate-Induced Testicular Damage

Reda F. A. Abdelhameed ^{1,2}, Shaimaa A. Fattah ³, Eman T. Mehanna ³, Dina M. Hal ¹, Sarah M. Mosaad ⁴, Maged S. Abdel-Kader ^{5,6,*}, Amany K. Ibrahim ¹, Safwat A. Ahmed ¹, Jihan M. Badr ¹ and Enas E. Eltamany ¹

¹ Department of Pharmacognosy, Faculty of Pharmacy, Suez Canal University, Ismailia 41522, Egypt

² Department of Pharmacognosy, Faculty of Pharmacy, Galala University, New Galala 43713, Egypt

³ Department of Biochemistry, Faculty of Pharmacy, Suez Canal University, Ismailia 41522, Egypt

⁴ Division of Pharmacology and Therapeutics, General Authority of Healthcare, Ismailia 41522, Egypt

⁵ Department of Pharmacognosy, College of Pharmacy, Prince Sattam Bin Abdulaziz University, Al-Kharj 11942, Saudi Arabia

⁶ Department of Pharmacognosy, Faculty of Pharmacy, Alexandria University, Alexandria 21215, Egypt

* Correspondence: m pharm101@hotmail.com; Tel.: +966-545-539-145



Citation: Abdelhameed, R.F.A.; Fattah, S.A.; Mehanna, E.T.; Hal, D.M.; Mosaad, S.M.; Abdel-Kader, M.S.; Ibrahim, A.K.; Ahmed, S.A.; Badr, J.M.; Eltamany, E.E. Zygo-Albuside A: New Saponin from *Zygophyllum album* L. with Significant Antioxidant, Anti-Inflammatory and Antiapoptotic Effects against Methotrexate-Induced Testicular Damage. *Int. J. Mol. Sci.* **2022**, *23*, 10799. <https://doi.org/10.3390/ijms231810799>

Academic Editor: Jae Youl Cho

Received: 15 August 2022

Accepted: 10 September 2022

Published: 16 September 2022

Publisher's Note: MDPI stays neutral with regard to jurisdictional claims in published maps and institutional affiliations.



Copyright: © 2022 by the authors. Licensee MDPI, Basel, Switzerland. This article is an open access article distributed under the terms and conditions of the Creative Commons Attribution (CC BY) license (<https://creativecommons.org/licenses/by/4.0/>).

Abstract: Chemical investigation of the crude extract of the aerial part of *Zygophyllum album* L. (*Z. album*) led to the isolation of a new saponin, Zygo-albuside A (7), together with seven known compounds, one of them (caffeic acid, compound 4) is reported in the genus for the first time. NMR (1D and 2D) and mass spectrometric analysis, including high-resolution mass spectrometry (HRMS), were utilized to set up the chemical structures of these compounds. The present biological study aimed to investigate the protective antioxidant, anti-inflammatory, and antiapoptotic activities of the crude extract from the aerial part of *Z. album* and two of its isolated compounds, rutin and the new saponin zygo-albuside A, against methotrexate (MTX)-induced testicular injury, considering the role of miRNA-29a. In all groups except for the normal control group, which received a mixture of distilled water and DMSO (2:1) as vehicle orally every day for ten days, testicular damage was induced on the fifth day by intraperitoneal administration of MTX at a single dose of 20 mg/kg. Histopathological examination showed that pre-treatment with the crude extract of *Z. album*, zygo-albuside A, or rutin reversed the testicular damage induced by MTX. In addition, biochemical analysis in the protected groups showed a decrease in malondialdehyde (MDA), interleukin-6 (IL-6) and IL-1 β , Bcl-2-associated-protein (Bax), and an increase in B-cell lymphoma 2 (Bcl-2) protein, catalase (CAT), superoxide dismutase (SOD) in the testis, along with an increase in serum testosterone levels compared with the unprotected (positive control) group. The mRNA expression levels of nuclear factor-kappa B (NF- κ B), tumor necrosis factor- α (TNF- α), p53, and miRNA-29a were downregulated in the testicular tissues of the protected groups compared with the unprotected group. In conclusion, the study provides sufficient evidence that *Z. album* extract, and its isolated compounds, zygo-albuside A and rutin, could alleviate testicular damage caused by the chemotherapeutic agent MTX.

Keywords: *Zygophyllum album* L.; saponins; antioxidant activity; antiapoptotic; testicular damage

1. Introduction

Methotrexate (MTX) is a folate antagonist that has been successfully used to treat various types of malignant tumors as well as autoimmune diseases [1]. One of the main obvious side effects of MTX cytotoxicity is damage to the testis, leading to sterility [2]. The latter has been associated with oxidative stress, inflammatory cytokines, and apoptotic cascades [3,4]. A close relationship has been established between MTX and oxidative stress, leading not only to an increase in reactive oxygen species (ROS) but also to a decrease in

antioxidant defense mechanisms such as antioxidant enzymes such as catalase (CAT) and superoxide dismutase (SOD) and non-enzymatic antioxidants such as reduced glutathione (GSH) [5–7]. Furthermore, inflammatory reactions in the male genital system are closely related to oxidative stress [8]. The pathogenesis of MTX-induced testicular damage is also associated with the production of proinflammatory cytokines such as interleukin-6 (IL-6) and IL-1 β and cell death via apoptotic cascades [3,6]. However, the exact processes that cause MTX-induced testicular damage are still unknown.

MicroRNAs (miRNAs) are short, non-coding RNAs of about 22 nucleotides that have been associated with the control of various physiological processes such as cell proliferation, cell death, fibrosis, inflammation, and metabolism [9–11]. The family of miRNA-29s consists of three members; miRNA-29a, miRNA-29b, and miRNA-29c. miRNA-29a is an important member of the miRNA-29 family and has been shown to exhibit proapoptotic activity [11,12]. Recently, administration of MTX showed upregulation of testicular miRNA-29a expression, which is associated with apoptosis, oxidative stress, and inflammation [13].

Several studies have proved that phytotherapeutic antioxidants are considered as an auspicious strategy for attenuating chemotherapy-induced organ toxicities [14–23]. Additionally, numerous natural products have been reported for being beneficial in the management of male reproductive problems [24] arising from environmental pollutants, toxins and drugs [25]. Various plant extracts and natural products have been evidenced to boost testosterone, improve the sperm quality, positively influence the androgen status, semen parameters and fertility index [26–30] as well as counteracting the gonadotoxicity induced by antineoplastic agents [13,24,25,31–33], D-galactose [34,35], heat [36,37] and radiation [38]. Such protective effects of the extracts are attributed to their antioxidant and anti-inflammatory components [13,24,25,31–38], most predominantly saponins [25,35–37]. Saponins are the most famous testosterone boosters that enhance testosterone production or function as antiestrogenic agents via aromatase or estrogen receptors inhibition [30]. They are responsible for the androgenic effect of *Tribulus terrestris* (Zygophyllaceae) [28]. Furthermore, date palm pollen saponins increased the testosterone production via the stimulation of Leydig cells of the testis [29]. The beneficial effects of ginseng on the male reproductive system are attributed to its saponin components known as ginsenosides [39]. Moreover, steroidal saponins of *Dioscorea* Genus (Yam) are used in the manufacture of steroidal hormones including sex hormones [40].

Zygophyllaceae (Caltrop family) comprises about 25 genera and 240 species among which six genera viz. *Tetradiclis*, *Seetzenia*, *Fagonia*, *Peganum*, *Tribulus* and *Zygophyllum album* (*Z. album*) are widespread in Egypt [41]. The genus *Z. album* is represented in Egypt by nine species [42,43], which are characterized by being succulent plants that resist drought and salt. These characters enable them to survive under drought, dry climatic situations [44]. Plants of genus *Zygophyllum* are employed by traditional healers in Egypt for the treatment of several ailments such as asthma, hypertension, diabetes, gout, rheumatism, and dysmenorrhea. Moreover, several biological studies evidenced their diverse pharmacological activities [43]. For instance, *Z. album* was reported to possess promising antioxidant [45–48], antidiabetic [46,47,49–51], antihyperlipidemic [47,49,52], anti-obesity [52], anti-acetylcholinesterase [52], antihypertensive [50], anticancer [47], cardioprotective and anti-inflammatory activities [53]. *Z. album* owes such pharmacological effects to an assortment of phytochemicals. Chemical investigation of *Z. album* revealed that the plant contains volatile oil [54] and accumulates triterpenes [43], saponins [43,55–58], sterols [43,55], phenolic compounds predominantly flavonoids [43,47,52,57,59], as well as few acids and their derivatives [52].

Based on the aforesaid considerations, besides that the impact of *Z. album* versus MTX-induced testicular injury has not been explored yet, we continued our efforts in discovering bioactive compounds from Egyptian folk medicine. Therefore, we investigated the chemical constituents of *Z. album* aerial parts and then studied the potential protective

effects of *Z. album* crude extract together with two of the isolated pure compounds against methotrexate-induced testicular damage.

2. Results

2.1. Structure Elucidation of the Isolated Compounds

The chemical structures of compounds 1–6 and 8 were identified based on co-chromatography with the available authentic samples and were further confirmed by comparing their ^1H NMR and ^{13}C NMR spectra data (Figures S1–S12, S30 and S31) with those previously reported in the literature. The chemical structures of the isolated compounds are displayed in Figure 1. Compound 1 was identified as β -sitosterol [60]. Compounds 2 and 3 were found to be triterpenes identified as β -amyrin and ursolic acid, respectively [61–63]. Compound 4 was characterized as caffeic acid [64]. Compounds 5, 6, and 8 were interpreted as flavonoids, namely kaempferol [65], quercetin [65,66], and rutin [67], respectively.

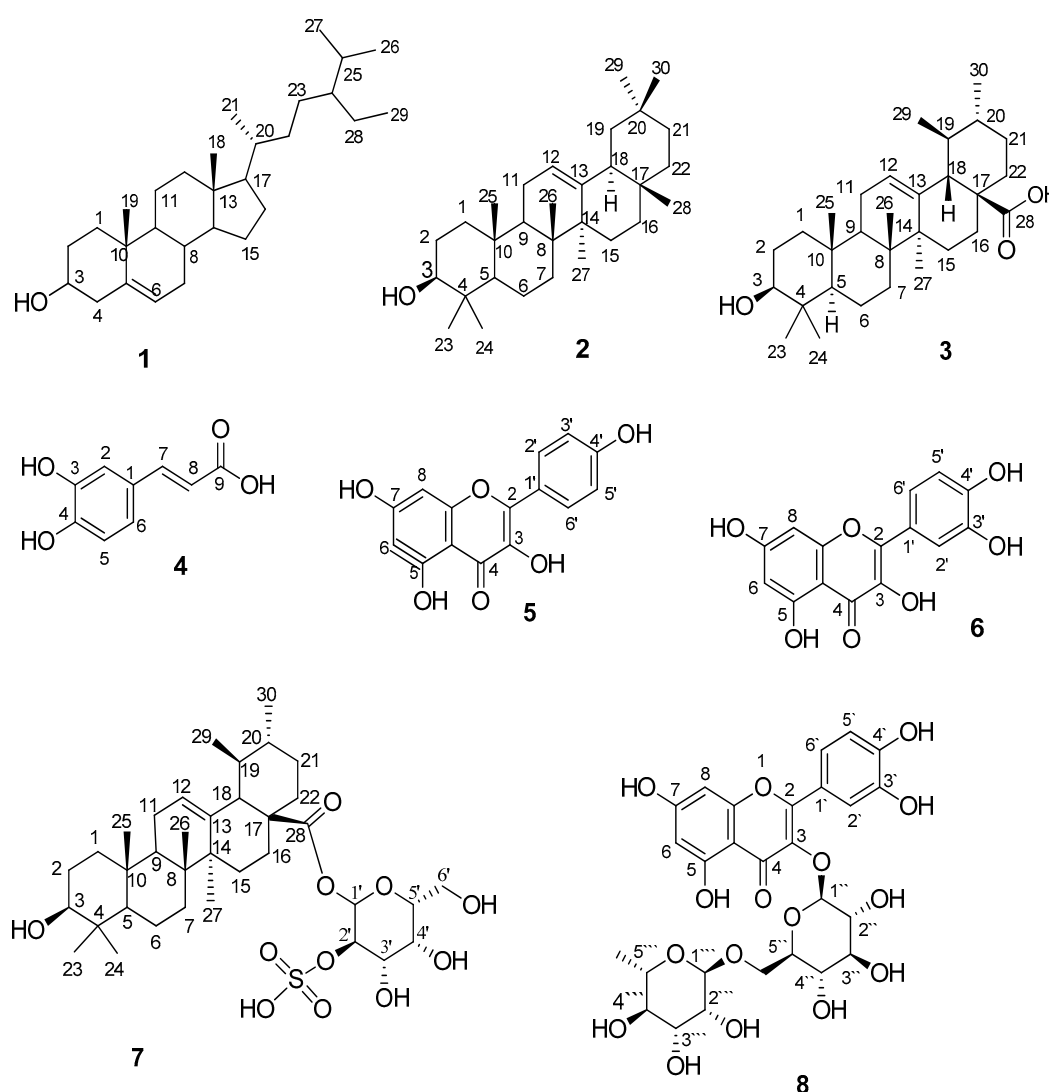


Figure 1. Chemical structures of the isolated compounds.

Compound 7 (Figures 1 and 2) was isolated as a white powder with a molecular formula of $\text{C}_{36}\text{H}_{58}\text{O}_{11}\text{S}$ as deduced from its ^1H and ^{13}C NMR spectral data (Table 1) and further confirmed by 2D NMR analysis and HRMS, which displayed a molecular ion peak at m/z 697.2885 $[\text{M}-\text{H}]^-$ (Figure S13). The positive results of rhodizonate test indicated the existence of a sulfate group [68–71].

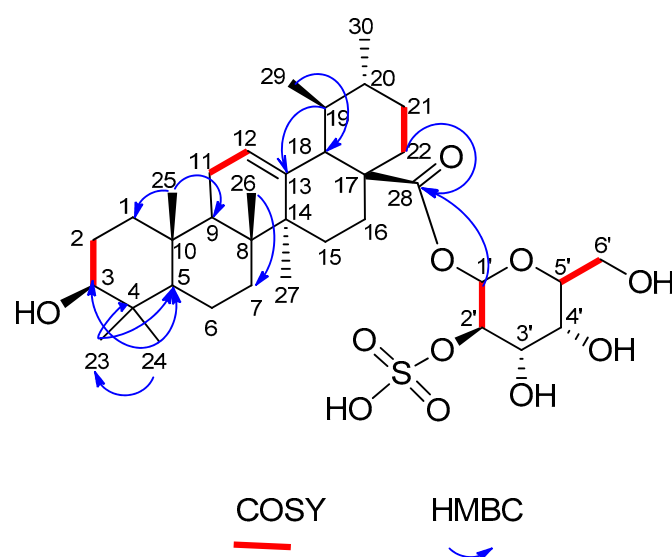


Figure 2. Selected COSY and HMBC correlations of compound 7.

Table 1. ^1H (500 MHz) and ^{13}C (125 MHz) NMR spectroscopic data of compound 7 (MeOH, δ in ppm, J in Hz).

No.	δ_C	δ_H (Int., Mult., J_{Hz})	No.	δ_C	δ_H (Int., Mult., J_{Hz})
1	39.0	1.10 (1H, m) 1.62 (1H, m)	19	38.6	1.11 (1H, m)
2	27.5	1.25 (1H, m) 1.42 (1H, m)	20	38.5	0.95 (1H, m)
3	74.9	3.64 (1H, dd, 5, 10)	21	30.8	1.02 (1H, m), 1.62 (1H, m)
4	38.9	-	22	37.7	1.41 (1H, m), 2.06 (1H, m)
5	55.6	0.95 (1H, m)	23	28.4	1.03 (3H, S)
6	19.9	0.95 (1H, m) 1.35 (1H, m)	24	19.9	0.93 (3H, S)
7	38.6	1.62 (1H, m) 1.73 (1H, m)	25	17.5	0.90 (3H, S)
8	40.4	-	26	19.9	1.00 (3H, S)
9	47.1	1.19 (1H, m)	27	13.6	1.10 (3H, S)
10	39.0	-	28	172.6	-
11	25.8	1.96 (1H, m), 2.15 (1H, m)	29	17.6	1.11 (1H, d, 10)
12	126.1	5.35 (1H, m)	30	21.4	0.94 (1H, d, 8)
13	138.5	-	1'	86.8	4.75 (1H, d, 10)
14	57.1	-	2'	78.5	4.07 (1H, dd, 5, 10)
15	28.4	1.03 (1H, m) 1.11 (1H, m)	3'	73.3	3.89 (1H, t, 5)
16	25.8	1.39 (1H, m) 2.16 (1H, m)	4'	68.9	4.08 (1H, m)
17	47.2	-	5'	74.6	3.65 (1H, m)
18	54.8	1.79 (1H, m)	6'	60.3	3.65 (1H, m) 3.89 (1H, m)

Extensive inspection of ^1H NMR and ^{13}C NMR data (Figures S14–S21) in addition to HSQC (Figures S27–S29) allowed for the assignment of five tertiary methyls detected at $\delta_{\text{H/C}}$ 0.90/17.5, 1.03/28.4, 1.00/19.9, 0.93/19.9 and 1.10/13.6 assignable for H_3/C -25, 23, 26, 24 and 27, respectively. This assignment was confirmed from HMBC correlations. For example, the signal detected a δ_{H} 0.93 assignable for H_3 -24 was correlated to the signal resonated at δ_{C} 28.4, 55.6 and 74.9 assignable for C-23, C-5 and C-3, respectively. The signal detected at δ_{H} 1.03 (for H_3 -23) was correlated to δ_{C} 38.9 and 55.6 assignable for C4 and C-5. In addition, the singlet at δ_{H} 0.90 (H_3 -25) was linked in HMBC spectrum

(Figures S25 and S26) to each of δ_C 39.0 and 47.1 assignable for C-1 and C-9, respectively. Similarly, other selected correlations are indicated in Figure 2.

The two methyls displayed at $\delta_{H/C}$ 0.94 (d, $J = 8.0$ Hz)/21.4 and 1.11 (d, $J = 10.0$ Hz)/17.6 were attributed to H₃-30/C-30 and H₃-29/C-29, respectively. Additionally, the oxygenated methine proton detected at δ_H 3.64 (dd, $J = 5, 10$ Hz) together with its corresponding carbon detected at δ_C 74.9 were assignable to H-3/C-3. The location of the hydroxyl group was further confirmed from the correlation between the singlet resonating at δ_H 0.93 (for H₃-24) and the carbon signal detected at δ_C 74.9 (for C-3). Moreover, H-3 (δ_H 3.64) was linked to H₂-2 (δ_H 1.25 and 1.42) as shown from the COSY spectrum (Figures S23 and S24).

An olefin proton was detected at $\delta_H = 5.35$ (m) attributed to H-12 with its corresponding carbon at δ_C 126.1 (C-12). Another sp² carbon resonated at δ_C 138.5, and this confirmed the classical double bond between C-12 and C-13. Another confirmation for the situation of the double bond was obtained from the COSY spectrum that revealed the link between H₂-11 (δ_H 1.96 and 2.15) and H-12 (δ_H 5.35). Additionally, HMBC spectrum illustrated correlation between C-13 (δ_C 138.5) and H-19 (δ_H 1.11).

The ¹³C NMR spectrum displayed resonances for characteristic signal at δ_C 172.6 for a carbonyl functionality of an ester; this signal disclosed a long range coupling with H₂-22 (δ_H 1.41 and 2.06) as exhibited by HMBC spectrum.

The DEPT-135 (Figure S22) allowed differentiation of the 36 carbon resonances into 7 methyl, 9 methylene, 7 methine, and 7 quaternary carbons attributed to the aglycon moiety. These data indicated an ursane-type triterpene skeleton for the aglycon with one carboxy group at C-28 [57,58,72]. The remaining six carbon signals were assigned to the sugar moiety which was identified as galactose. ¹³C NMR spectra displayed the characteristic signal of an anomeric carbon at δ_C 86.8, which appeared shielded due to the presence of the -SO₃H group at C-2'. The anomeric carbon for galactose usually appears around 99.2 [73], but in the presence of the -SO₃H group at C-2', it moves up the field to 86.8 [72]. The remaining signals at δ_C 78.5, 73.3, 68.9, 74.6, and 60.3 indicate the presence of a sugar part.

The anomeric proton exhibited a coupling constant at δ_H 4.75 (1H, d, $J = 10.0$ Hz, H-1'), which is characteristic to the di-axial interaction between H-1' and H-2'; this value, besides the chemical shift of the anomeric carbon at δ_C 86.8, assured the β -configuration [74–76].

The situation of the sugar moiety was indicated from the long-range coupling between the anomeric proton resonating at δ_H 4.75 and the carbonyl functionality detected at δ_C 172.6 as revealed from the HMBC spectrum. To place emphasis on the structure of compound 7, it was subjected to acid hydrolysis [77] followed by co-chromatography of the resulted aglycone and sugar parts of compound 7 with authentic triterpenes and sugars, respectively. The aglycone part was assured to be ursolic acid (compound 3) ($R_f = 0.3, 0.64$ and 0.71 mobile phase: benzene/toluene (1:4), toluene/EtOAc/AcOH (6:3:1) and 3% MeOH in CHCl₃ [78–80]). The sugar moiety was authenticated to be galactose ($R_f = 0.21, 0.38$ and 0.39 ; mobile phase: *n*-butanol-benzene-pyridine-HO (5:1:3:3), PhOH satd. with H₂O and propanol-H₂O (8.5:1.5), respectively) [81,82].

Based on the above including the ¹H and ¹³C NMR data, which were compared with those previously published for Zygophyllum saponins [57,58,83] and confirmed by HMBC and COSY correlations (Figure 2), compound (7) was elucidated as a new compound isolated for the first time from a natural source and given the name Zygo-albuside A.

2.2. In Vitro Antioxidant Assessment of Compound 7 (Zygo-Albuside A)

Plant antioxidants frame a wide assortment of phytochemicals that exert their antioxidant action by various mechanisms such as including quenching of singlet oxygen, hydrogen convey, transport of electron in addition to reduction of metal and chelation [84,85]. Previous studies have proven the antioxidant activity of *Z. album* different extracts and fractions [46,48,86,87]. This encouraged the inspection of the antioxidant efficacy of compound 7 (Zygo-albuside A) in the current study by utilizing three indicative assays (DPPH, H₂O₂, TAC).

The DPPH radical has been frequently utilized to explore the neutralizing effects of crude extracts or pure compounds. Antioxidants can pause the free radicals' chain of oxidation reactions via creating more stable radicals. Thus, they can scavenge the DPPH radical through donation of hydrogen, giving rise to transformation of the purple-colored DPPH radical into the yellow-colored DPPH-H [88,89].

In this study, the results depicted in Table 2 revealed that compound 7 possessed promising radical scavenging ability with $IC_{50} = 45.41 \pm 2.65 \mu\text{g/mL}$ compared to ascorbic acid as positive control ($IC_{50} = 10.64 \pm 0.82 \mu\text{g/mL}$).

Table 2. In vitro antioxidant activities of compound 7 by DPPH, H_2O_2 and TAC assays.

Sample	DPPH (IC_{50} in $\mu\text{g/mL}$)	H_2O_2 (IC_{50} in $\mu\text{g/mL}$)	TAC (mg GAE/g)
Compound 7	45.41 ± 2.65	65.16 ± 3.22	29.83 ± 2.19
Ascorbic acid	10.64 ± 0.82	NT	71.28 ± 4.34

NT, not tested. Data are expressed as mean \pm SD of three independent values.

Furthermore, hydrogen peroxide (H_2O_2) is a powerful oxidant, playing a decisive role in cell signaling pathways [89]. In biological systems, H_2O_2 is produced by a number of oxidizing enzymes such as SOD [90]. However, the accumulation of H_2O_2 can cause oxidative stress and inflammatory reactions [89,91,92]. Decomposition of H_2O_2 into the hydroxyl radical ($\bullet\text{OH}$) initiates lipid peroxidation and causes cellular components injury, giving rise to several inflammatory conditions [93]. Accordingly, controlling H_2O_2 production by natural antioxidants could be of great benefit [89]. Compound 7 exhibited good H_2O_2 quenching effect with an $IC_{50} = 65.16 \pm 3.22$ (Table 2).

The in vitro total antioxidant capacity (TAC) of compound 7 was assessed by application of phosphomolybdate assay, which depends on the generation of a green phosphate/MoV complex. This complex is created due to the reduction of phosphomolybdate ion by the compound with an antioxidant effect [84]. Results were expressed as milligram of gallic acid equivalent per gram of dry extract (mg GAE/g).

Accordingly, compound 7 exhibited noteworthy TAC (29.83 ± 2.19 mg GAE/g) matched with ascorbic acid (the positive control; 71.28 ± 4.34 mg GAE/g) pointing to its potent capacity to remove free radicals by an electron transfer mechanism (Table 2).

2.3. In Vivo Evaluation of *Z. album* Extract, Compound 7 (Zygo-Albuside A) and Compound 8 (Rutin)

2.3.1. Effect on Liver and Kidney Function Markers (Preliminary Study)

In order to assess the possible toxicity of the administered compounds on the liver and kidney, a preliminary study was conducted to determine the serum levels of the liver enzymes alanine aminotransferase (ALT), and aspartate aminotransferase (AST), and the kidney markers urea and creatinine in mice that received only *Z. album* extract (100 mg/kg), zygo-albuside A (10 mg/kg) and rutin (10 mg/kg). No significant differences were observed in the levels of both liver and kidney function markers in any of the treated groups relative to the negative control mice (Table S1), indicating that the investigated doses had no detected toxicity on either the liver or the kidney (Table S1). No other toxic effects were detected in the experimental mice. There were also no observed changes in the behavior of the treated mice nor a marked increase in their mortality rates.

2.3.2. Reversing Serum Testosterone Levels in the MTX-Administrated Mice

The results in Figure 3A show that administration of MTX in the principle investigative study was associated with a significant 73% decrease in serum testosterone levels compared with the normal control (NC) group. MTX-injected mice pretreated with either the crude extract of *Z. album*, zygo-albuside A, or rutin showed a significant increase in serum testosterone levels by 33%, 42.8%, and 47.8% compared to the untreated MTX (positive control) group.

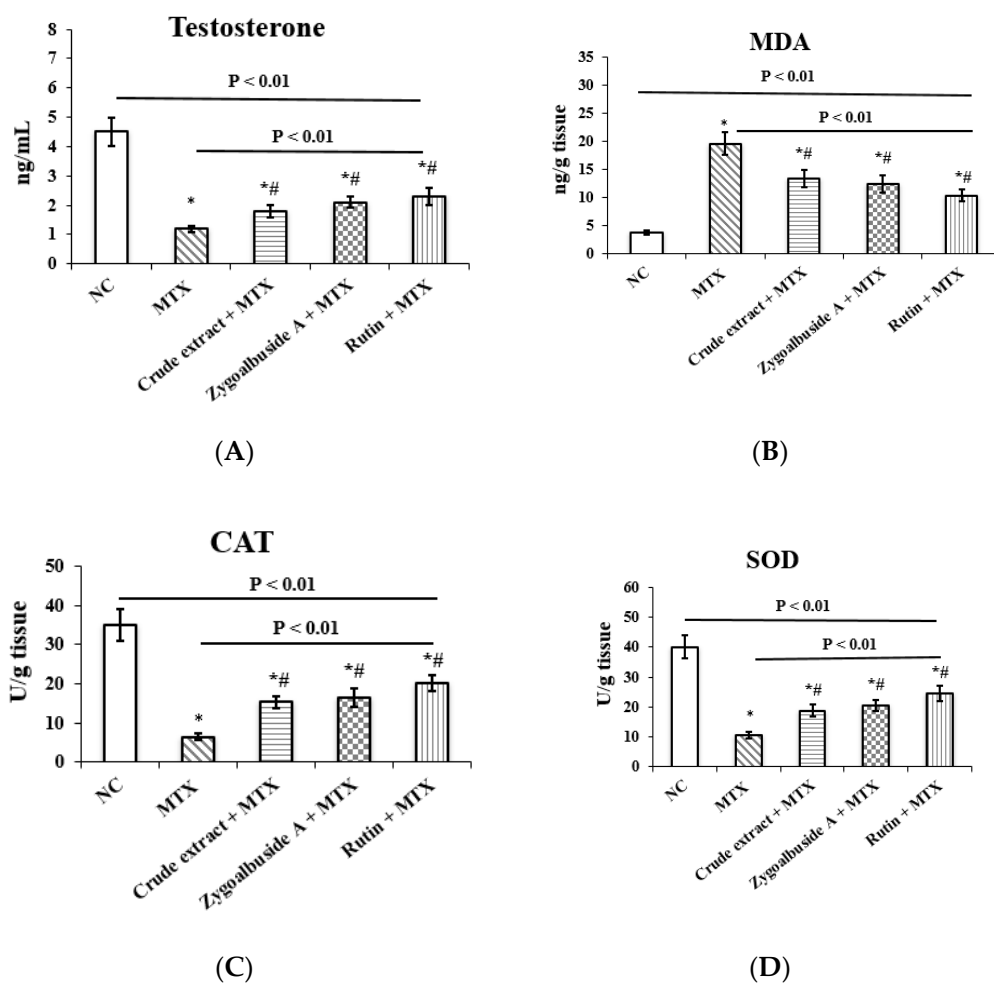


Figure 3. Effect of administration of *Z. album* crude extract, zygo-albuside A and rutin on serum levels of (A) testosterone, and testicular levels of (B) MDA, (C) CAT and (D) SOD in MTX-induced testicular injury mice. Statistical analysis was performed using ANOVA followed by Tukey's post hoc test. Values are expressed as mean \pm SD (n = 8). A statistically significant difference was assumed at $p < 0.01$ and denoted by * vs. NC; # vs. MTX. MDA; malondialdehyde, CAT; catalase, SOD; superoxide dismutase.

2.3.3. Restoring the Antioxidant Activity in the MTX-Administrated Mice

As shown in Figure 3B, testicular malondialdehyde (MDA) levels were significantly increased by 80.6% in the MTX group compared with the NC group. Co-administration of *Z. album* crude extract, zygo-albuside A, or rutin with MTX significantly decreased testicular tissue MDA levels by 31.6%, 36.7%, and 46.9%, respectively, compared with the MTX positive control group.

Compared with NC, a significant decrease in the activities of CAT and SOD (73.5% and 81.4%, respectively) was observed after exposure to MTX. Concurrent treatment with *Z. album* crude extract, zygo-albuside A, or rutin showed significant restoration of the levels of these testicular antioxidants compared with mice injected with MTX alone (Figure 3C,D).

2.3.4. Reduction of Inflammation in the MTX-Administrated Mice

MTX administration was associated with significant inflammatory changes in testicular tissue, as indicated by significant increases in the expression levels of nuclear factor-kappa B (NF- κ B), tumor necrosis factor- α (TNF- α) by 8.9- and 9.2-fold, respectively, and a significant increase in IL-1 β and IL-6 levels by 80.7%, and 81.7%, respectively, compared with the NC group (Figure 4A–D).

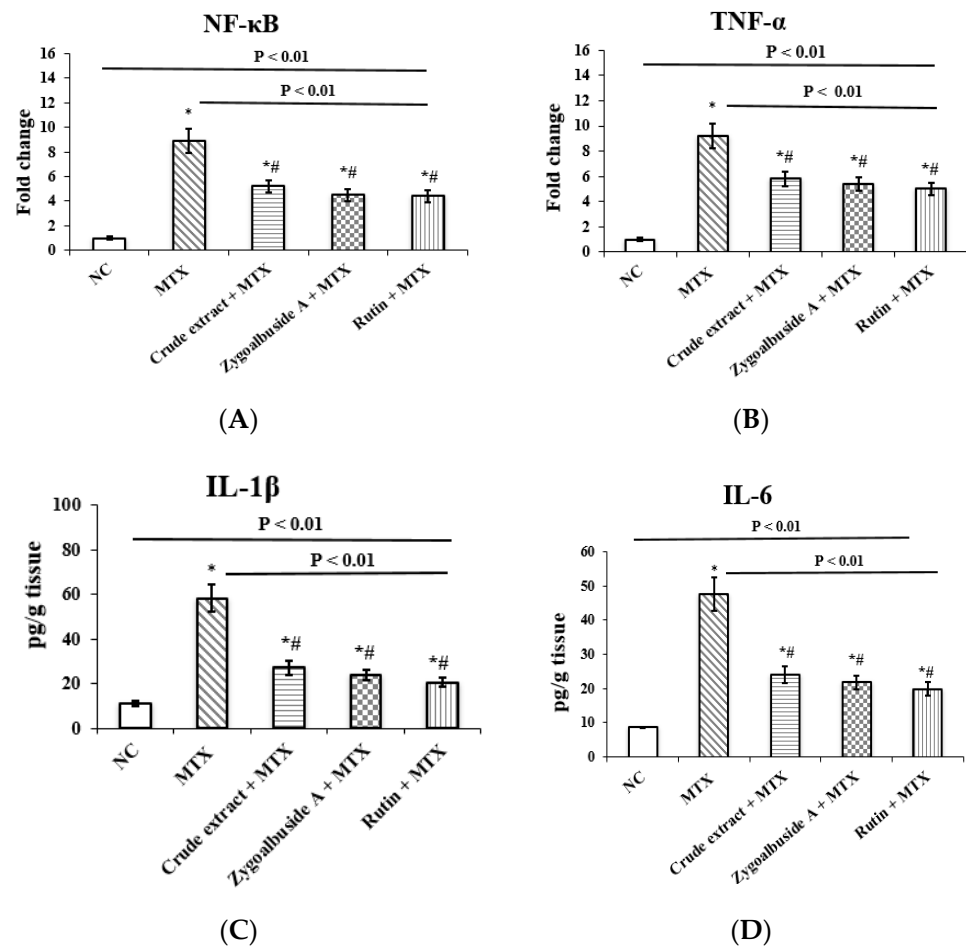


Figure 4. Testicular gene expression of (A) NF-κB, (B) TNF-α and tissue levels of (C) IL1-β and (D) IL-6 in the normal control (NC) group and experimental groups (MTX, crude extract + MTX, zygo-albuside A + MTX, rutin + MTX). Statistical analysis was performed using ANOVA followed by Tukey's post hoc test. Values are expressed as mean ± SD (n = 8). A statistically significant difference was assumed at $p < 0.01$ and denoted by * vs. NC; # vs. MTX. NF-κB; nuclear factor kappa B, TNF-α; tumor necrosis factor-α, IL-1β; interleukin-1β, IL-6; interleukin-6.

MTX-injected mice pretreated with either *Z. album* crude extract, zygo-albuside A, or rutin showed significant decreases in NF-κB expression levels by 5.2-, 4.5-, and 4.4-fold, respectively, and in TNF-α expression levels by 5.8-, 5.4-, and 5-fold, respectively, compared with the unprotected (positive control) group. Apparently, the isolated compounds also had a significant effect on IL-1β and IL-6 levels by decreasing them compared to the MTX positive control group. *Z. album* crude extract, zygo-albuside A, or rutin exhibited a significant decrease in IL-1β levels by 53.3%, 59.1%, and 64.6%, respectively, and in IL-6 levels by 49.3%, 53.9%, and 58.4%, respectively (Figure 4A–D).

2.3.5. Prevention of Apoptosis in the MTX-Administrated Mice

In response to cellular stress, the tumor suppressor p53 leads to cell cycle arrest and apoptosis [94]. In this context, administration of MTX resulted in a significant 8.5-fold increase in p53 expression in the testis compared to the NC group. This effect was attenuated by pre-administration of *Z. album* crude extract, zygo-albuside A, or rutin by 4.9-, 3.7-, and 3.3-fold, respectively, compared to the MTX positive control group (Figure 5A).

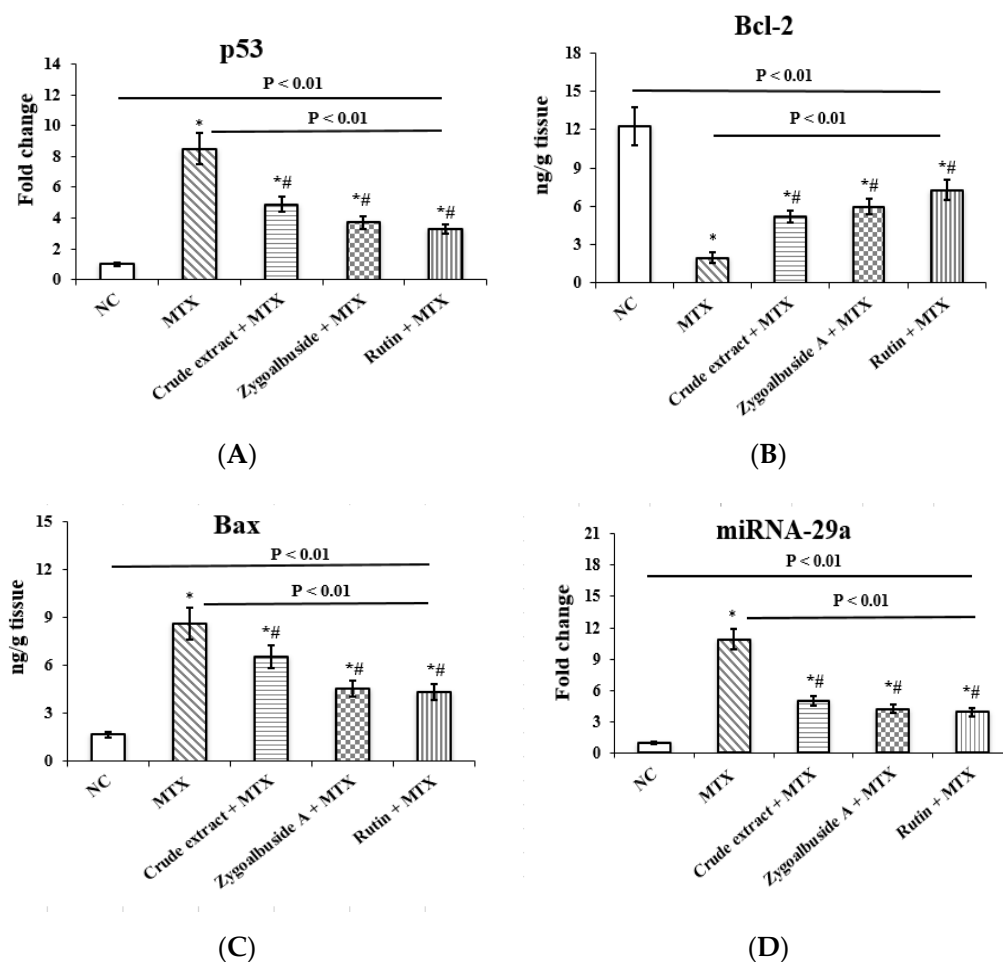


Figure 5. Effect of administration of crude extract, zygo-albuside A, or rutin on testicular expression of (A) p53, (B) miRNA-29a, mRNA and testicular levels of (C) Bax and (D) Bcl-2 in mice with MTX-induced testicular injury. Statistical analysis was performed using ANOVA followed by Tukey's post hoc test. Values are expressed as mean \pm SD ($n = 8$). A statistically significant difference was assumed at $p < 0.01$ and denoted by * vs. NC; # vs. MTX.

Members of the Bcl-2 family play an important role in testicular cell survival by regulating both caspase-dependent and caspase-independent cell death. Bcl-2 is an anti-apoptotic protein belonging to the family of apoptosis-regulating proteins [95]. The current results showed that only MTX-injected mice had 83.9% lower Bcl-2 levels than the NC group. Mice pretreated with *Z. album* crude extract, zygo-albuside A or rutin had 62%, 67% and 72% higher Bcl-2 levels, respectively, compared to the MTX positive control group (Figure 5B).

Furthermore, Bax levels were significantly increased by 81% in mice administered MTX only compared with the NC group. Pretreatment with *Z. album* crude extract reduced Bax levels by 24% compared with untreated mice. Stronger effects were apparently caused by zygo-albuside A or rutin, which reduced Bax levels by 47% and 45%, respectively, compared with the MTX positive control group (Figure 5C).

2.3.6. Inhibition of mi-RNA 29a Expression in MTX-Administrated Mice

The expression of mi-RNA 29a was significantly increased by 10.9-fold in MTX-injected mice relative to the NC group. Oral administration of *Z. album* crude extract, Zygo-albuside A, or rutin significantly decreased mi-RNA 29a expression by 54%, 61%, and 64%, respectively, compared with the MTX positive control group (Figure 5D).

2.3.7. Improvement of the Histological Damage in the Testis

As shown in Figure 6, a normal structure was observed in the testis of the control mice, and the mice receiving zygo-albuside A and rutin exhibited normal architecture of the testicular tubules with complete spermatogenesis. In contrast, the group injected with MTX (positive control group) showed hyalinized tubules with a significant decrease in spermatogenesis compared to the NC group. In addition, a significant decrease in Johnsen score in the group injected with MTX was observed compared to the normal testicular parts. Treatment with *Z. album* crude extract improved the Johnsen score nine-fold compared with the unprotected group. Maximum protection was achieved by zygo-albuside A and rutin compounds, which brought the score to normal.

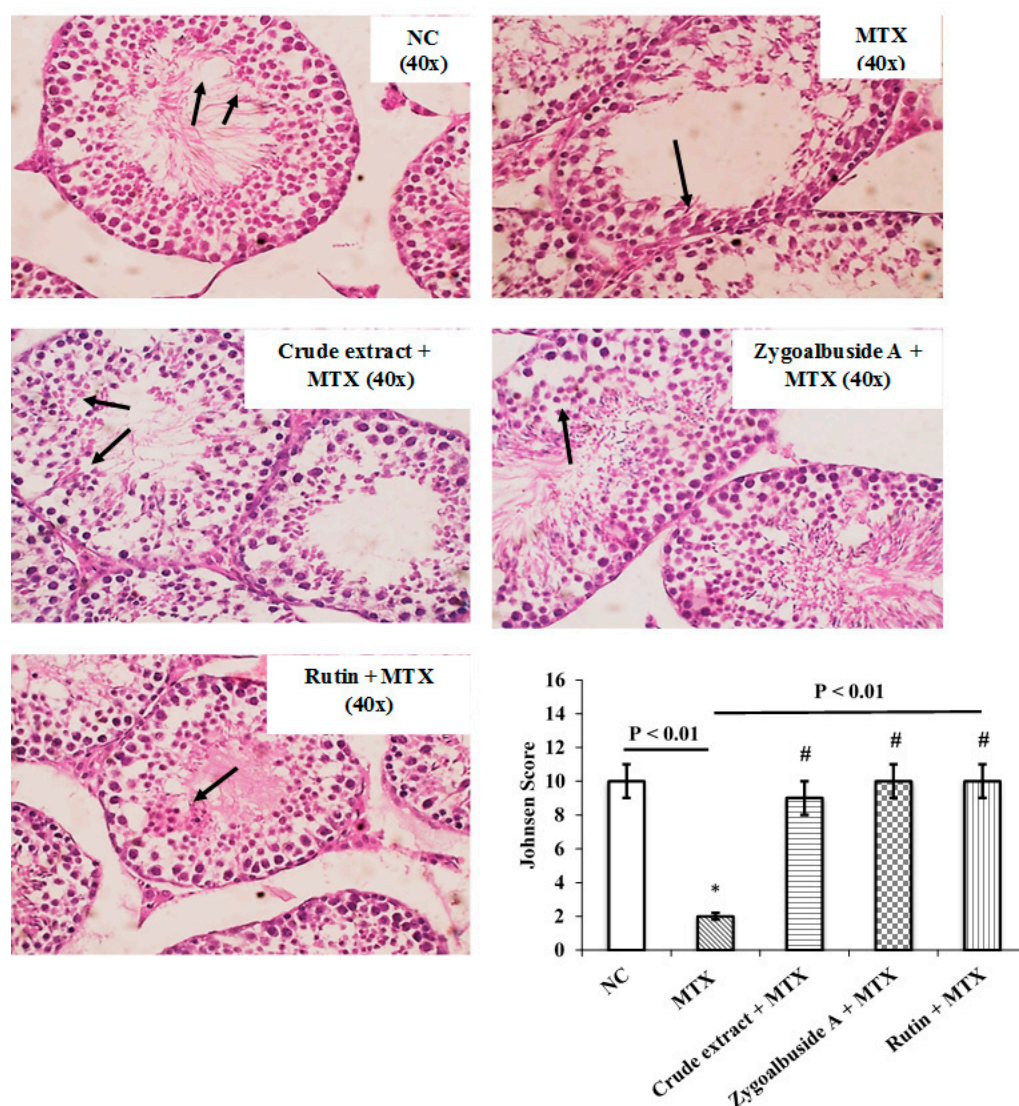


Figure 6. Representative photomicrographs of testis from control and experimentally treated mice. Testicular tissue sections stained with hematoxylin and eosin (40 \times) and scored by Johnsen. The normal control group (NC) showed complete spermatogenesis (black arrow) in all tubules, up to the sperm count (score 10). In the MTX group, some tubules are hyalinized, while other tubules show a marked reduction in spermatogenesis with few spermatocytes (black arrows) (score 2). The Crude extract + MTX group showed tubules with complete spermatogenesis (black arrows) and slightly impaired spermatogenic cells (score 9). The Zygo-albuside A + MTX group showed the most pronounced effect; complete spermatogenesis is evident in all tubules up to spermatids (black arrow) (score 10). The Rutin + MTX group also showed complete spermatogenesis in all tubules, up to the

spermatids (black arrow) (score 10). Scores are expressed as mean \pm SD (n = 8). Statistical analysis was performed by one-way analysis ANOVA followed by Tukey's post hoc test. A statistically significant difference was assumed at $p < 0.01$ and marked with * vs. NC; # vs. MTX.

3. Discussion

Chemotherapeutic drugs have always been associated with persistent azoospermia and infertility in men. MTX can damage testicular tubules, reduce sperm count, and cause genetic abnormalities [96]. Consistent with previous studies, the present study found that a single i.p. dose of 20 mg/kg MTX can cause testicular damage. In this context, great attention should be paid to these side effects, and new natural products should be sought to counteract MTX-induced testicular damage.

Our histological findings showed damage to testicular tissue with hyalinized testicular tubules and a significant decrease in the Johnsen score for spermatogenesis after injection of MTX compared with NC. Consequently, MTX resulted in a significant decrease in testosterone levels compared with NC. Several research papers supported our findings demonstrating the reproductive toxicity of MTX [13,34,96].

It is reported that the toxicity of MTX is triggered by several mechanisms, including oxidative stress, inflammation, and apoptosis [35,55,97]. Exposure to X-rays, toxins, and chemicals in the environment, as well as certain physical disorders such as varicocele, can increase oxidative stress and promote germ cell death and thus spermatogenesis [98]. Sperm abnormalities and infertility are caused by uncontrolled ROS production and oxygen-induced lipid peroxidation of the abundant polyunsaturated fatty acids in the sperm membrane [99,100]. In this regard, tissue levels of MDA, a marker of lipid peroxidation [5], were increased in the MTX group compared to NC. In addition, the MTX group showed a significant decrease in testicular levels of the antioxidant enzymes SOD and CAT compared to NC; similar results were previously observed [13,96,97]. The body's ability to produce antioxidants under normal circumstances to counteract the negative effects of oxidative stress is influenced by metabolic processes and genetic structure. In addition, environmental variables such as diet, pollution, and chemicals can affect this ability. As a result, the body's antioxidant system cannot neutralize all free radicals and prevent the harmful effects of oxidative stress alone [98].

Furthermore, previous studies have shown that MTX-induced testicular injury is associated with a marked increase in pro-inflammatory cytokines [3,6,101,102]. An increase in TNF- α and/or IL-1 β following testicular injury activates the JNK pathway, a stress-related kinase that plays an important role in inflammatory diseases [103] and controls the maturation and function of T cells as well as the production of ROS and pro-inflammatory cytokines such as IL-6 and TNF- α [101]. Moreover, binding of TNF to TNFR1 induces degradation of I κ B α , triggering the canonical NF- κ B signaling mechanism that activates proinflammatory cytokine genes such as IL-6 and IL-1 β [104]. In this regard, previous studies have shown that NF- κ B can be stimulated by TNF- α in Sertoli cells [101]. In agreement with previous studies, our results have shown that injection of MTX led to a significant increase in testicular levels of IL-6 and IL-1 β , which may be reflected by the upregulation of NF- κ B and an increase in TNF- α expression in the testis, compared with NC.

Apoptosis has also been implicated in the pathophysiology of MTX-induced gonadotoxicity [4]. Apoptosis is triggered by either the receptor-mediated extrinsic pathway or the mitochondria-dependent intrinsic mechanism. The extrinsic pathway is activated when extracellular apoptosis-inducing stimuli such as TNF- α dock to death receptors and activate the initiator caspase 8. Members of the Bcl-2 family with anti- or pro-apoptotic activities, such as Bcl-2 and Bax, control the mitochondria-dependent intrinsic pathway. Bcl-2 can prevent cell death by preserving the integrity of the mitochondrial membrane and blocking cytochrome c release. Bax furthermore translocates into mitochondria and promotes the release of cytochrome c, eventually leading to the activation of initiator caspase 9. Both initiator caspases can then activate executioner caspase 3, leading to apoptotic

cell death [105]. Sheikhabaei et al. [4] found that DNA damage induced after injection of MTX activates the p53 gene, which in turn enhances Bax expression. Consistent with the previous studies [4,13,106], the present study demonstrated significantly decreased Bcl-2 levels in MTX-treated mice compared with the NC group. In addition, the expression of p53 and Bax levels were significantly increased in the testicular tissues of the MTX-group compared with the NC group.

Upregulation of miRNA-29 family expression, particularly miRNA-29a, was reported in testis by injection of estradiol benzoate and doxorubicin, both of which promote germ cell apoptosis [107]. Members of the miRNA-29 family have been shown to induce apoptosis in a p53-dependent manner [108]. The present study agrees with the study by Sherif et al. [13] in which the group treated with MTX showed significant miRNA-29a expression compared to NC. Other previous studies have identified a molecular pathway linking miRNA-29a overexpression to oxidative stress activation via increased MDA and decreased SOD levels [12]. Moreover, overexpression of miR-29a increased the production of IL-6 and IL-1 as well as NF- κ B activation [109].

Considering that oxidative stress, inflammation, and apoptosis caused by MTX are serious problems that lead to organ failure and have been shown to damage the male reproductive system, the present study aimed to investigate whether oral treatment with *Z. album* extract and two of its isolated compounds can alleviate testicular damage induced by MTX in mice. We investigated a new natural product isolated from *Z. album*, zygo-albuside A, which showed promising protective effects against MTX-induced testicular damage. In addition, various protective effects of *Z. album* crude extract or rutin against testicular damage were observed. In the groups injected with MTX and pretreated with *Z. album* crude extract, zygo-albuside A, or rutin, histopathological examination showed complete spermatogenesis in all tubules compared to the positive control MTX-injected mice.

The present study revealed the structural characterization of the new compound zygo-albuside A obtained from *Z. album*. Zygo-albuside A is a saponin consisting of a sugar moiety glycosidically linked to a hydrophobic aglycone. Saponin is one of the most popular structures among natural products used in traditional medicine against various disease mechanisms. In this context, saponin from *Agave brittoniana* Trel subspecies *brachypus* showed anti-inflammatory activity [110]. Moreover, a previous study elucidated the anti-inflammatory effect of saponins from the roots of *Impatiens parviflora* DC [111]. In the present study, histopathological improvement of testicular tissue and increases in testosterone levels were associated with significant downregulation of NF- κ B and TNF- α mRNA and decreases in testicular levels of IL-1 β and IL-6 in the zygo-albuside A-treated group. Similar histopathological improvements and anti-inflammatory effects were observed in the groups treated with the crude extract of *Z. album* and rutin. The anti-inflammatory properties of *Z. album* have been previously described as cardioprotective, and hepatoprotective [55] effects were previously reported, mainly through suppressing the NF- κ B pathway. Moreover, rutin was postulated to exert anti-inflammatory effects via inhibition of the NF- κ B signaling pathway [112]. Based on the current results, we propose that the *Z. album* crude extract, zygo-albuside A, and rutin may have anti-inflammatory effects by suppressing the activation of NF- κ B along with the pro-inflammatory cytokines IL-1 β , IL-6, and TNF- α .

Saponins that protect against oxidative stress have received increased attention. It is known from the literature that Notoginsenoside R1 may be able to repair cell damage in neurons by suppressing ROS [113]. Moreover, ginsenoside Rg1 protected human neuroblastoma cells from hydrogen peroxide-induced damage [114]. Consistent with these findings, the present study showed that the saponin zygo-albuside A reduced MTX-induced testicular damage by restoring normal levels of testicular antioxidant enzymes such as SOD and CAT and by decreasing testicular MDA levels compared with the MTX positive control group. The same results were obtained for rutin and the crude extract of *Z. album*. These results agree with previous reports on *Z. album* [55]. This could be due to its flavonoid content. Vardi et al. [5] reported the effect of flavonoids on lowering serum MDA and NO

and increasing SOD and CAT. Rutin specifically was reported to protect against testicular ischemia–reperfusion-induced oxidative stress in rats through decreasing MDA and increasing SOD and CAT activities [115]. The study by Alsharif et al. [116] reported that inhibition of the action of TNF- α ameliorated dexamethasone-induced oxidative stress in mice. Therefore, we hypothesize a relationship between the anti-inflammatory effect of *Z. album* extracts and their antioxidant capacity.

Furthermore, ginsenoside Rb1 showed an anti-apoptotic effect in *Rattus* pancreatic β -cells via decreasing caspase-3 gene expression [117]. In addition, the high flavonoid content of some natural products contributes to their anti MTX effect by suppressing various apoptotic pathways and DNA damage [4,5,34]. In the current study, the zygo-albuside A saponin as well as the rutin flavonoid showed anti-apoptotic effect by significantly reducing p53 mRNA expression in the testis with concomitant reduction in Bax and an increase in Bcl-2 levels. More to the point, a previous study showed that TNF- α and IL-6 levels are inversely correlated with Bcl-2 expression [118]. Moreover, antioxidants inhibit apoptosis by downregulating p53 and caspase enzymes [119]. Consequently, the current results suggest that the anti-inflammatory effect of the isolated compounds of *Z. album* is not only related to their antioxidant activity, but also to their anti-apoptotic effect in the treatment of testicular damage caused by MTX.

Several natural products have been shown to be highly effective drugs for treatment of a variety of clinical conditions through their influence on miRNA expression [120,121]. Consistent with previous findings, oral administration of the crude extract of *Z. album*, the new natural product zygoalbusid A, or rutin attenuated testicular damage caused by injection of MTX by downregulating testicular miRNA-29a whose anti-inflammatory, antioxidant, and anti-apoptotic effects have been demonstrated in previous studies [99,122,123].

Overall, Figure 7 summarizes the mechanisms of the protection provided by the new saponin zygo-albuside A against MTX-induced testicular injury.

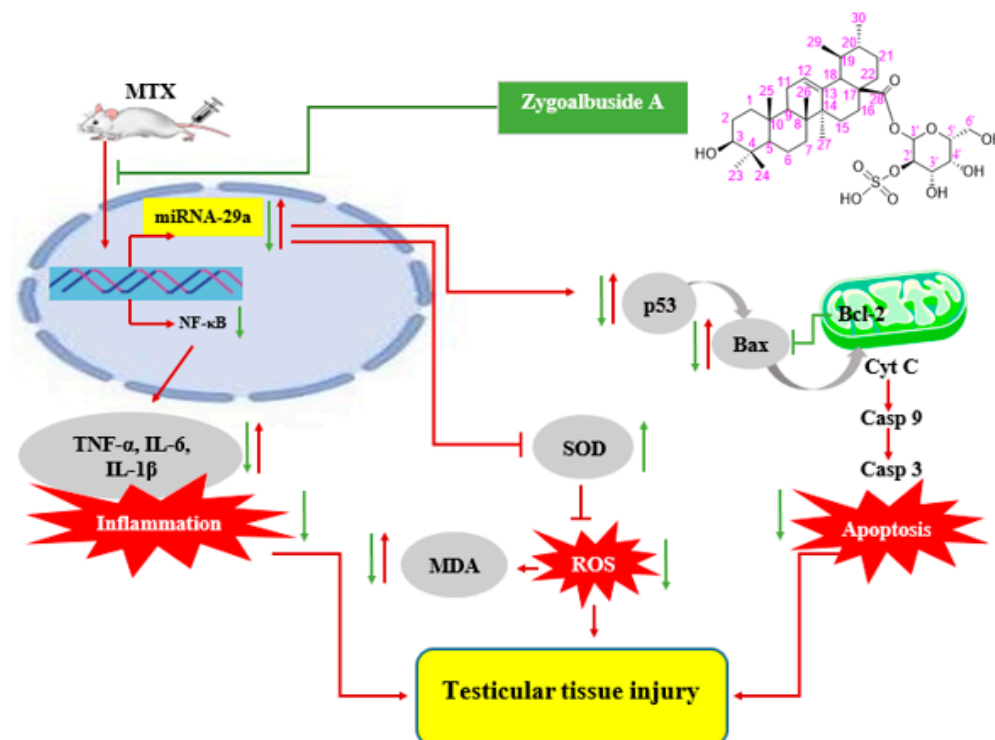


Figure 7. Protective mechanism of zygo-albuside A against methotrexate-induced testicular damage. Red arrows indicate the effects of MTX injection. Green arrows indicate the effects of zygo-albuside A administration. MTX; methotrexate, NF- κ B; nuclear factor kappa B, TNF- α ; tumor necrosis factor- α , IL-1 β ; interleukin 1 β , IL-6; interleukin-6, SOD; superoxide dismutase, ROS; reactive oxygen species, MDA; malondialdehyde, Cyt C; cytochrome C, Casp; caspase.

4. Materials and Methods

4.1. General Experimental Procedures

First, 1D and 2D NMR spectra (chemical shifts in ppm, coupling constants in Hz) were reported using Bruker Avance DRX 500 MHz spectrometers (Billerica, MA, USA). HRMS were measured through direct injection by Thermo Scientific UPLC RS Ultimate 3000-Q Exactive (Thermo Fisher Scientific, Waltham, MA, USA) hybrid quadrupole-Orbitrap mass spectrometer combined with high-performance quadrupole precursor selection with high resolution, accurate mass Orbitrap™ detection. Detection was performed in both negative and positive modes. Chromatographic separation was performed using columns packed with Sephadex LH-20 (0.25–0.1 mm, Pharmacia, Sigma-Aldrich, St. Louis, MI, USA) and silica gel 60 (0.04–0.063 mm). Precoated TLC plates (with silica gel 60 F254, 0.2 mm, Merck, Kenilworth, NJ, USA) and Whatman™ Grade 1 Chr Cellulose Chromatography Paper (Sigma-Aldrich, St. Louis, MI, USA) were used for detection of the chemical components. Spots were visualized using UV absorption at λ of 255 and 366 nm, in addition to spraying with *p*-anisaldehyde/H₂SO₄. Aniline phthalate reagent was used for visualization of sugar spots. Reference standards of β sitosterol ($\geq 95\%$), β amyryn (phyproof®, $\geq 90\%$), ursolic acid ($\geq 90\%$), caffeic acid ($\geq 98\%$), kaempferol ($\geq 97\%$), quercetin ($\geq 95\%$), rutin (phyproof®, $\geq 95\%$), D-glucose ($\geq 99.5\%$), D-galactose ($\geq 99\%$) were purchased from (Sigma-Aldrich, St. Louis, MI, USA).

4.2. Plant Material

Z. album was collected from Marsa Matrouh at the Northern Coast of the Mediterranean in Egypt during May 2019. It was identified at the Faculty of Science, Alexandria University. A voucher specimen was kept under registration number ZA-2019 in the herbarium of Pharmacognosy Department, Faculty of Pharmacy, Suez Canal University, Ismailia, Egypt.

4.3. Extraction and Isolation

First, 1.8 kg of the chopped small pieces of aerial parts of plant *Z. album* was extracted with methanol (3 × 2 L) at room temperature. The combined extract was concentrated under reduced pressure to give brownish green viscous crude extract (50 g).

The crude extract (45 g, suspended in 1 L. distilled water) was partitioned using *n*-hexane, CHCl₃, EtOAc and *n*-BuOH to give five fractions (ZA-1–ZA-5) that were concentrated under reduced pressure. Fraction ZA-1 (100% *n*-hexane) (5 g) was applied on a silica gel column, 100% *n*-hexane was used for elution then gradient systems of *n*-hexane: EtOAc: MeOH, until reaching EtOAc: MeOH (50:50) to give ten subfractions (ZA-1-a to ZA-1-j). Subfraction (ZA-1-b) (610 mg) was chromatographed on silica gel and eluted by EtOAc: hexane starting with 5% EtOAc in hexane to 100% EtOAc followed by a Sephadex LH-20 column using CHCl₃: MeOH (1:1) to finally acquire compound 1 (6.5 mg, white waxy substance). Subfraction (ZA-1-f) (550 mg) was similarly chromatographed on silica gel (the eluting system was EtOAc in hexane; 5% EtOAc in hexane to finally 100% EtOAc). Sephadex LH-20 column was applied for final purification using isocratic elution (CHCl₃: MeOH; 1:1) to obtain compound 2 (3 mg, white powder).

Fraction ZA-2 (100% CHCl₃) (6 g) was partitioned on a silica gel column and eluted with 10% EtOAc in *n*-hexane and then by gradient systems of *n*-hexane, EtOAc and MeOH until reaching 50% EtOAc in MeOH. This yielded nine subfractions (ZA-2-a to ZA-2-i). Subfraction (ZA-2-c) (990 mg) was applied on silica gel using gradient systems of EtOAc in hexane starting with 10% EtOAc in hexane to 100% EtOAc. Sephadex LH-20 column (with eluting mixture CHCl₃: MeOH; 1:1) was set for final purification to acquire compound 3 (7 mg, creamy-white powder).

Fraction ZA-3 (100% EtOAc) (10 g) was added on a silica gel column, eluted with 100% CHCl₃ and then by gradient systems (CHCl₃ and MeOH until 50% MeOH in CHCl₃); four subfractions (ZA-3-a to ZA-3-d) were obtained. Subfraction (ZA-3-a) (1.3 g) was purified on silica gel using elution by 100% CHCl₃ then CHCl₃: MeOH until 50% MeOH

in CHCl_3 . This afforded three subfractions (ZA-3-a-1 to ZA-3-a-3). Subfraction (ZA-3-a-2) (250 mg) was treated similarly on silica gel (gradient systems: 100% CHCl_3 then CHCl_3 : MeOH until 100% MeOH). Final purification was performed using Sephadex LH-20 column and CHCl_3 : MeOH (1:1) for isocratic elution to afford compound 4 (18 mg, colorless gum substance).

Subfraction (ZA-3-b) (1 g) was fractionated on silica gel column, eluted by gradient systems of 100% CHCl_3 and MeOH until 50% MeOH in CHCl_3 . This afforded four subfractions (ZA-3-b-1 to ZA-3-b-4). Subfraction (ZA-3-b-1) (270 mg) was purified using silica gel and gradient systems of CHCl_3 : MeOH starting with 10% MeOH in CHCl_3 until 100% MeOH. The purification was completed by a Sephadex LH-20 column and CHCl_3 : MeOH (1:1) for isocratic elution to obtain compound 5 (5 mg, yellowish powder).

Subfraction (ZA-3-c) (1 g) was treated in a similar way using silica gel column, eluted initially by 100% CHCl_3 , followed by gradient systems of CHCl_3 : MeOH until (1:1) CHCl_3 : MeOH to yield three subfractions (ZA-3-c-1 to ZA-3-c-3). Subfraction (ZA-3-c-3) (320 mg) was added on silica gel where gradient systems of CHCl_3 : MeOH were applied. (10% MeOH in CHCl_3 until 100% MeOH). The last step in purification was performed using Sephadex LH-20 column and CHCl_3 : MeOH (1:1) to yield compound 6 (3 mg, yellowish powder).

Subfraction (ZA-3-d) (2.5 g) was chromatographed on silica gel using initially 100% CHCl_3 and then with gradient systems of CHCl_3 : MeOH until (1:1) CHCl_3 : MeOH, which yielded four subfractions (ZA-3-d-1 to ZA-3-d-4). Subfraction (ZA-3-d-1) (350 mg) was added on silica gel using gradient systems (CHCl_3 : MeOH starting with 10% MeOH in CHCl_3 until 100% MeOH), where two subfractions (ZA-3-d-1-a and ZA-3-d-1-b) were obtained. Subfraction (ZA-3-d-1-b) (180 mg) was purified on silica gel using gradient systems of CHCl_3 : MeOH starting with 10% MeOH in CHCl_3 until 100% MeOH, and then, a Sephadex LH-20 column was applied for final purification using CHCl_3 : MeOH (1:1) to obtain compound 7 (65 mg, white powder).

Subfraction (ZA-3-d-4) (670 mg) was purified similarly using silica gel column and CHCl_3 with gradual increase in MeOH (10% MeOH in CHCl_3 until 100% MeOH); followed by a Sephadex LH-20 column using CHCl_3 : MeOH (1:1) to obtain pure compound 8 (60 mg, yellowish powder).

4.4. Acid Hydrolysis of Compound 7

Following the method described in [77], a quantity of 5 mg of compound 7 was hydrolyzed by 2 N HCl (1 mL) at 95 °C. The reaction mixture was then diluted with water and then extracted with CHCl_3 , and the recovered aglycone was subjected to PC and TLC co-chromatography with compound (3) and a standard sample of ursolic acid using benzene/toluene (1:4) [78], toluene/EtOAc/ AcOH (6:3:1) [79] and 3% methanol in CHCl_3 [80] as mobile phases.

The aqueous phase after usual work-up procedure yielded D-galactose identified by comparison with authentic sugars using silica gel TLC and propanol- H_2O (8.5:1.5) as a developer [81], as well as PC applying *n*-butanol-benzene-pyridine- H_2O (5:1:3:3) and PhOH satd. with H_2O as mobile phases [82]. Sugar spots were visualized by aniline phthalate reagent.

4.5. Detection of the Sulfate Group

As described in [68], 5 mg of compound 7 was refluxed with 5 mL of HCl (2N) for 2 h and then neutralized with dil NaOH. The reaction mixture was then dried under vacuum. The residue was subjected to paper chromatography using 90% MeOH dried in air then sprayed with BaCl_2 solution (100 mg in 50 mL of 70% MeOH), The paper was then air dried and finally sprayed with potassium rhodizate solution (10 mg dissolved in 50 mL of 50% MeOH). A yellow color indicated the presence of sulfate group.

4.6. Spectroscopic Data of the Isolated Compounds

4.6.1. Compound (1) ($R_f = 0.25, 0.41$ and 0.83 ; Mobile Phase: 25% EtOAc in Hexane, $\text{CHCl}_3/\text{MeOH}/\text{AcOH}$ (97:2:1) and Petroleum Ether/ $\text{CHCl}_3/\text{MeOH}$ (49:50:1), Respectively [80,124,125])

^1H NMR ($\text{C}_5\text{D}_5\text{N}$, 500 MHz): δ_{H} 1.01 (H-1a, m, H-1), 1.83 (H1b, m, H-1), 1.46 (2H, m, H-2), 3.52 (1H, dd, 5, 10, H-3), 2.21 (H-4a, m, H-4), 2.31 (H4b, m, H-4), 5.35 (1H, m, H-6), 1.85 (2H, m, H-7), 1.35 (1H, m, H-8), 0.85 (1H, m, H-9), 1.44 (H-11a, m, H-11), 1.49 (H11b, m, H-11), 1.13 (H-12a, m, H-12), 1.95 (H12b, m, H-12), 1.07 (1H, m, H-14), 1.18 (H-15a, m, H-15), 1.23 (H15b, m, H-15), 1.16 (2H, m, H-16), 1.00 (1H, m, H-17), 0.68 (3H, s, H-18), 0.92 (3H, s, H-19), 1.32 (1H, m, H-20), 0.84 (3H, d, $J = 6.6$, H-21), 1.28 (H-22a, m, H-22), 1.07 (H22b, m, H-22), 1.53 (2H, m, H-23), 1.53 (2H, m, H-23), 0.85 (1H, m, H-24), 1.64 (1H, m, H-25), 0.80 (3H, d, $J = 6.6$, H-26), 0.84 (3H, d, $J = 7.2$, H-27), 1.18 (H-28a, m, H-28), 1.23 (H28b, m, H-28), 0.80 (3H, t, $J = 7.2$, H-29).

^{13}C NMR (MeOD, 125 MHz): δ_{C} 11.9 (C-29), 12.0 (C-24), 18.8 (C-28), 19.4 (C-19), 19.9 (C-27), 21.1 (C-11, C-26), 23.1 (C-23), 24.3 (C-15), 26.0 (C-21), 28.3 (C-16), 29.1 (C-25), 31.9 (C-2, C-7, C-8), 33.9 (C-20), 36.2 (C-18), 36.5 (C-10), 37.3 (C-1, C-12), 42.2 (C-13), 42.5 (C-4), 45.8 (C-22), 50.1 (C-9), 56.0 (C-17), 56.8 (C-14), 71.8 (C-3), 121.7 (C-6), 140.7 (C-5).

4.6.2. Compound (2) ($R_f = 0.39, 0.57$ and 0.58 ; Mobile Phase: 25% EtOAc in Hexane, $\text{CHCl}_3/\text{MeOH}$ (97:3) and Toluene/ MeOH (9:1) and, Respectively [80,126,127])

^1H NMR (CDCl_3 , 300 MHz) at δ : 0.69, 0.76, 0.85, 0.87, 0.90, 0.95, 1.16, 1.19 (each 3H, s, C-25, C-23, C-30, C-29, C-24, C-26, C-27, C-28), 3.62 (dd, $J = 10, 5$ Hz, H-3) 5.73 (d, $J = 7.2$ Hz, H-12).

^{13}C NMR (CDCl_3 , 125 MHz): δ_{C} 14.4 (C-24), 14.4 (C-25), 17.3 (C-26), 17.4 (C-6), 20.0 (C-11), 22.7 (C-30), 22.7 (C-27), 24.5 (C-16), 25.6 (C-15), 26.3 (C-2), 27.0 (C-23), 28.6 (C-28), 29.9 (C-20), 31.8 (C-7), 33.3 (C-17), 33.2 (C-29), 34.4 (C-21), 35.3 (C-10), 35.2 (C-22), 37.1 (C-4), 37.5 (C-1), 39.9 (C-8), 41.8 (C-14), 47.3 (C-9), 48.5 (C-19), 49.5 (C-18), 54.5 (C-5), 78.2 (C-3), 122.9 (C-12), 145.9 (C-13).

4.6.3. Compound (3) ($R_f = 0.30, 0.64$ and 0.71 ; Mobile Phase: Benzene/Toluene (1:4), Toluene/EtOAc/AcOH (6:3:1) and 3% MeOH in CHCl_3 , Respectively [78–80])

^1H NMR ($\text{C}_5\text{D}_5\text{N}$, 500 MHz): δ_{H} 1.03 (H-1a, m, H-1), 1.57 (H1b, m, H-1), 1.81 (2H, m, H-2), 3.44 (1H, dd, 5, 10, H-3), 0.87 (1H, m, H-5), 1.36 (H-1a, m, H-6), 1.57 (H1b, m, H-6), 1.36 (H-1a, m, H-7), 1.57 (H1b, m, H-7), 1.67 (1H, m, H-9), 1.96 (2H, m, H-11), 5.48 (1H, s, H-12), 1.27 (H-1a, m, H-15), 2.13 (H1b, t, 10, H-15), 2.14 (1H, t, 10, H-16), 2.02 (1Hb, m, H-16), 2.63 (1H, d, 10, H-18), 1.47 (1H, m, H-19), 1.05 (1H, m, H-20), 1.44 (1Ha, m, H-21), 1.52 (1Hb, m, H21), 1.94 (2H, m, H-22), 1.28 (3H, s, H-23), 1.03 (3H, s, H-24), 0.94 (3H, s, H-25), 1.05 (3H, s, H-26), 1.27 (3H, s, H-27), 1.03 (3H, s, H-29), 0.97 (3H, d, 10, H-30).

^{13}C NMR ($\text{C}_5\text{D}_5\text{N}$, 125 MHz): δ_{C} 15.5 (C25), 16.4 (C24), 17.2 (C26, C29), 18.6 (C-6), 21.2 (C30), 23.6 (C27), 23.7 (C-11), 28.1 (C-2), 28.5 (C23), 28.6 (C-15), 32.9 (C21), 33.1 (C-7), 37.0 (C22), 37.1 (C-10), 38.7 (C20), 39.2 (C-1, C19), 39.5 (C-4), 41.8 (C-8), 42.3 (C-14), 47.1 (C-16), 47.8 (C17), 47.9 (C-9), 53.3 (C18), 55.6 (C-5), 77.9 (C-3), 122.3 (C-12), 144.6 (C-13), 179.9 (C28).

4.6.4. Compound (4) ($R_f = 0.35, 0.79$ and 0.96 ; Mobile Phase: Toluene/EtOAc/HCOOH (6:3:1), *n*-Butanol/AcOH/ H_2O (4:1:5) and EtOAc/AcOH/HCOOH/ H_2O (100:11:11:26), Respectively [79,82,128])

^1H NMR (MeOD, 500 MHz): δ_{H} 7.45 (1H, d, $J = 16.0$ Hz, H-7), 6.94 (1H, d, $J = 1.5$ Hz, H-2), 6.85 (1H, dd, $J = 8.0, 1.5$ Hz, H-6), 6.69 (1H, d, $J = 8.0$ Hz, H-5), 6.14 (1H, d, $J = 16.0$ Hz, H-8).

^{13}C NMR (MeOD, 125 MHz): δ_{C} 126.4 (C-1), 114.2 (C-2), 145.6 (C-3), 148.1 (C-4), 115.1 (C-5), 121.5 (C-6), 145.4 (C-7), 113.7 (C-8), 169.7 (C-9).

4.6.5. Compound (5) (R_f = 0.26, 0.55 and 0.58; Mobile Phase: Toluene/EtOAc/HCOOH (7:3:0.1), Forestal = conc. HCl/AcOH/H₂O (3:30:10) and PhOH/H₂O (3:1), Respectively [82,129])

^1H NMR (DMSO-*d*₆, 500 MHz): δ_{H} 6.18 (1H, d, J = 2 Hz, H-6), 6.44 (1H, s), 8.04 (1H, dd, J = 2.8, 8.5 Hz, H-2'), 6.94 (1H, dd, J = 2.7, 10 Hz, H-5'), 8.04 (1H, dd, J = 2.7, 11.6 Hz, H-6'), 6.94 (1H, dd, 2.7, 8.5, H-3').

^{13}C NMR (DMSO-*d*₆, 125 MHz): δ_{C} 147.2 (C-2), 136.1 (C-3), 176.3 (C-4), 161.2 (C-5), 98.7 (C-6), 164.4 (C-7), 93.9 (C-8), 156.6 (C-9), 103.5 (C-10), 122.1 (C-1'), 129.9 (C-2'), 115.9 (C-3'), 159.6 (C-4'), 115.9 (C-5'), 129.9 (C-6').

4.6.6. Compound (6) (R_f = 0.29, 0.41 and 0.9; Mobile Phase: PhOH/H₂O (3:1), Forestal = conc. HCl/AcOH/H₂O (3:30:10) and EtOAc/AcOH/H₂O (7.5:1.5:1.5), Respectively [80,130])

^1H NMR (DMSO-*d*₆, 500 MHz): δ_{H} 6.20 (1H, d, J = 2 Hz, H-6), 6.42 (1H, d, J = 2 Hz, H-8), 7.70 (1H, d, J = 2.2 Hz, H-2'), 6.90 (1H, d, J = 8.5 Hz, H-5'), 7.56 (1H, dd, J = 8.5, 2.2 Hz, H-6'), 9.41 (1H, s, H-4'), 9.35 (1H, s, H-3'), 12.49 (1H, s, H-3), 12.52 (1H, s, H-5), 12.49 (1H, s, H-7).

^{13}C NMR (DMSO-*d*₆, 125 MHz): δ_{C} 147.2 (C-2), 136.2 (C-3), 176.2 (C-4), 156.6 (C-5), 98.7 (C-6), 164.3 (C-7), 93.8 (C-8), 161.6 (C-9), 103.5 (C-10), 122.5 (C-1'), 116.0 (C-2'), 145.5 (C-3'), 148.1 (C-4'), 115.5 (C-5'), 120.8 (C-6').

4.6.7. Compound (7) (R_f for the aglycone (R_f = 0.30, 0.64 and 0.71 Mobile Phase: Benzene/Toluene (1:4), Toluene/EtOAc/AcOH (6:3:1) and 3% MeOH in CHCl₃, Respectively. [78–80]. R_f for the Sugar Part = 0.21 0.38 and 0.39; Mobile Phase: *n*-Butanol/Benzene/Pyridine/H₂O (5:1:3:3), PhOH satd. with H₂O and Propanol/H₂O (8.5:1.5), respectively) [79,80])

White powder; HRMS: m/z 697.2885 [M-H][−]; ^1H NMR (MeOH, 500 MHz) and ^{13}C NMR (MeOH, 125 MHz) spectral data, see Table 1.

4.6.8. Compound (8) (R_f = 0.24, 0.28 and 0.45; Mobile Phase: EtOAc/AcOH/HCOOH/H₂O (100:10:10:18), EtOAc/AcOH/H₂O (7.5:1.5:1.5) and EtOAc/AcOH/HCOOH/H₂O (100:11:11:26) [130–132])

^1H NMR (DMSO-*d*₆, 500 MHz): δ_{H} 6.20 (1H, d, J = 2 Hz, C6-H), 6.40 (1H, d, J = 2 Hz, C8-H), 7.55 (1H, s, C2'-H), 6.87 (1H, d, J = 8.5 Hz, C5'-H), 7.55 (1H, s, C6'-H), 12.59 (1H, s, C5-OH), 5.35 (1H, s, H1''), 3.40 (1H, m, H2'', H5''), 3.30* (1H, m, H3''), 3.28* (1H, m, H4''), 3.41* (1H, m, H6''), 3.84 (1H, m, H6''), 5.15 (1H, d, J = 1.9, H1'''), 3.62* (1H, m, 2'''), 3.60* (1H, m, 3'''), 3.30* (1H, m, 4'''), 3.42* (1H, m, 5'''), 1.00 (3H, d, J = 6.1, CH₃-6''').

^{13}C NMR (DMSO-*d*₆, 125 MHz): 18.2 (C6'''), 67.4 (C6''), 68.7 (C5'''), 70.4 (C4'''), 70.8 (C2'''), 71.0 (C3'''), 72.3 (C4''), 74.5 (C2''), 76.3 (C5''), 76.8 (C3''), 94.1 (C-8), 99.2 (C-6), 101.2 (C1'''), 101.6 (C1''), 104.4 (C-10), 115.7 (C-2'), 116.7 (C-5'), 121.6 (C-6'), 122.1 (C-1'), 133.7 (C-3), 145.2 (C-3'), 148.8 (C-4'), 157.1 (C-2, C-5), 161.6 (C-9), 164.5 (C-7), 177.9 (C-4).

4.7. In Vitro Antioxidant Assay of Compound 7

4.7.1. DPPH Radical Scavenging Activity

The method was applied as previously published [133]. The measurements proceeded as the average of triplicates. The percentage of inhibition (PI) of the DPPH radical was deemed based on the formula:

$$\text{PI} = \left[\frac{(\text{AC} - \text{AT})}{\text{AC}} \times 100 \right] \quad (1)$$

where AC = absorbance of the control at t = 0 min, and AT = absorbance of the compound 7 + DPPH at t = 16 min.

IC₅₀ is the concentration needed to 50%; DPPH radical scavenging activity was calculated from graphic plots of the dose response curve using Graphpad Prism software (San Diego, CA, USA) [134].

4.7.2. Hydrogen Peroxide Radical (H₂O₂) Scavenging Activity

The test was performed based on the previously published procedure [135]. BHT was the reference standard. The H₂O₂ radical scavenging percentage of compound 7 was estimated by the following equation:

$$\text{H}_2\text{O}_2 \text{ radical scavenging percentage} = [(A_{\text{blank}} - A_{\text{sample}}) / A_{\text{blank}}] \times 100 \text{ g extract}$$

IC₅₀ was estimated from graphic plots of the dose–response curve using Graphpad Prism software (San Diego, CA, USA).

4.7.3. Total Antioxidant Capacity (TAC)

Total antioxidant capacity of compound 7 was evaluated by the phosphomolybdate complex method [136]. TAC was measured (as mg equivalents gallic per 100 g compound 7) using the standard gallic graph.

4.8. In Vivo Investigation of the Protective Effects of *Z. album* Extract, Compound 7 and Compound 8 against MTX-Induced Testicular Injury

4.8.1. Preliminary Assessment of the Liver and Kidney Toxicity

A total of 20 mice (20–30 g) were randomly divided into 4 groups (5 mice each). The first group received the vehicle (distilled water:DMSO (2:1)) and was considered the normal group. The other three groups received *Z. album* extract (100 mg/kg), zygo-albuside A (10 mg/kg) and rutin (10 mg/kg), respectively. The determined doses were administered orally for 7 consecutive days. Blood samples were collected from the mice after 7 days and serum was separated. Serum levels of the liver function enzymes ALT and AST were assessed by colorimetric kits; AL1031 and AS1061, respectively (Biodiagnostic, Giza, Egypt). Similarly, the serum levels of the kidney markers urea and creatinine were also determined calorimetrically; UR2110 and CR1250, respectively (Biodiagnostic, Giza, Egypt).

4.8.2. Animals and Treatment (the Principle In Vivo Study)

The current in vivo investigative study was performed on 40 male Swiss albino mice of the same age with an initial average body weight of approximately 20–30 g. The minimum number of animals required to achieve statistical significance was used, and every effort was made to minimize animal suffering. These mice were bred at the “Animal Sector” of the Egyptian Biological Products and Vaccines Organization (Vacsera, Giza, Egypt). The mice were kept in aluminum cages at controlled room temperature (25 °C). All animal handling was approved by the Ethical Committee of the Faculty of Pharmacy, Suez Canal University (202010PHDA₁). After a two-week acclimation period, the animals were randomly divided into five groups (8 mice each). The mice in the first group received a mixture of distilled water and DMSO (2:1) as vehicle orally every day for ten days and served as the NC group (Group I). In the remaining mice, testicular damage was induced on the fifth day by a single intraperitoneal (i.p.) dose of 20 mg/kg methotrexate (MTX) [137]. These mice were randomly divided into four groups: Group II (MTX positive control group): Mice received only MTX; Group III (crude extract + MTX): Mice were received 100 mg/kg crude extract of *Z. album* [138]; Group IV (Zygo-albuside A + MTX): Mice received 10 mg/kg zygo-albuside A [139]; Group V (Rutin + MTX): Mice received 10 mg/kg rutin [140].

Z. album crude extract, zygo-albuside A, and rutin were administered daily by oral gavage for the total period of the experiment (i.e., 10 days).

4.8.3. Tissue Collection

Mice were sacrificed by decapitation under ketamine anesthesia at the end of the 10-day treatment. Blood samples were collected for serum separation in plain vacutainers. Testis were removed, weighed, and decapsulated, and a portion of the tissue was stored at $-80\text{ }^{\circ}\text{C}$ for biochemical analysis. Another part of the testis was placed in formalin solution (10%) for histopathological studies.

4.8.4. Biochemical Analysis

Measurement of Testosterone

The level of testosterone levels (cat. no. MBS263193) was determined in serum by ELISA kit (MyBioSource, San Diego, CA, USA).

Determination of the Level of Oxidative Stress in the Testis

One gram of testis was homogenized in 2 mL of ice-cold phosphate-buffered saline (PBS) lyses buffer (pH = 7.4) using a disintegrator (Ultra-Turrax homogenizer, Darmstadt, Germany). The homogenate was then centrifuged at $3000 \times g$ for 15 min, and the supernatant obtained was frozen in aliquots at $-80\text{ }^{\circ}\text{C}$ until analysis. The levels of MDA, SOD, and CAT in the testis were determined using mice-specific ELISA kits (San Diego, CA, USA; Cat. No. MBS741034, MBS034842, and MBS160589, respectively).

Determination of Testicular Inflammation and Apoptosis Mediators

Levels of IL-1 β , IL-6, Bax, and Bcl-2 were determined in the homogenate samples of testicular tissue by mice-specific ELISA kits according to the manufacturer's instructions ELISA kit (MyBioSource, San Diego, CA, USA; cat. no. MBS701092, MBS762321, MBS763832-, and MBS2512543, respectively).

Determination of Testicular Expression of NF- κ B, TNF- α , p53, and miR-29a by Quantitative Real-Time Polymerase Chain Reaction

The Qiagen miRNeasy Mini Kit (cat. no. 217004) was used to separate total RNA, including miRNA, from testicular tissue (Qiagen, Hilden, Germany). NanoDrop spectrophotometer was used to determine the concentration and purity of the extracted RNA (Thermo Fisher Scientific, Waltham, MA, USA).

Expression levels of NF- κ B, TNF- α , p53, and miR-29a were measured in testicular tissue using GoTaq[®] 1-Step RT-qPCR technology (Promega, Madison, WI, USA). The endogenous control for NF- κ B, TNF- α , and p53 was β -Actin, whereas miR-29a was controlled by small nuclear RNA U6B (RNU6B). The primers and annealing temperatures are listed in (Table S2). For the experiment, 4 μL of RNA template, 0.4 μL of GoScript[™] RT mix for 1-step RT-qPCR, 1 μL of forward and reverse primers, 10 μL of GoTaq[®] qPCR master mix, 0.31 μL of additional CXR reference dye, and 3.29 μL of nuclease-free water were used. Cycles included 15 min of reverse transcription at $37\text{ }^{\circ}\text{C}$, 10 min of reverse transcriptase enzyme inactivation at $95\text{ }^{\circ}\text{C}$, and 40 cycles of denaturation at $95\text{ }^{\circ}\text{C}$ for 10 s, annealing for 30 s, and extension at $72\text{ }^{\circ}\text{C}$ for 30 s. The StepOnePlus[™]Real-Time PCR Thermal Cycler was used for all real-time PCR experiments (Applied Biosystems, Waltham, MA, USA). The $\Delta\Delta\text{Ct}$ and fold change values were determined, and the results were expressed as the mean fold change compared with the NC group.

4.8.5. Histological Analysis

For histological examination, testicular tissue was cut into tiny slices and fixed in 10% buffered formalin before being treated with a graded ethanol series, embedded in kerosene, and finally cut into 2–3 m thick slices. Hematoxylin and eosin (H&E) stains were used for regular histological assessment. An Olympus microscope (Shinjuku, Japan) equipped with a spot digital camera and MATLAB software computer program was used for observation, and specimens were photographed. To evaluate the histopathological changes, the Johnsen scoring system was used to calculate the degree of seminiferous

tubules. Depending on the presence of spermatogenic cells, the system was scored as the followings: 1, absence of seminiferous epithelium; 2, no germinal cells; 3, only spermatogonia; 4, there are no spermatozoa or spermatids and only a few spermatocytes; 5, no spermatozoa or spermatids, but many spermatocytes; 6, there are no spermatozoa, no late spermatids, and only a few early spermatids; 7, no spermatozoa, no late spermatids, but plenty of early spermatids; 8, spermatozoa per tubule, with few late spermatids; 9, somewhat disrupted spermatogenesis, several late spermatids, and disordered epithelium; 10, full spermatogenesis [98].

4.8.6. Statistical Analysis

Data were analyzed using Statistical Package for Social Sciences (SPSS) software, version 17 (Chicago, IL, USA) SPSS. Results were presented as mean \pm SD. Significant differences between treatment effects were determined by one-way analysis of variance (ANOVA) followed by Bonferroni's post hoc multiple comparison test, with statistical significance level set at <0.01 .

5. Conclusions

The current study afforded the isolation and structure elucidation of a new saponin; zygo-albuside **A**, along with seven known compounds from *Z. album* areal parts. The study demonstrated for the first time that administration of isolated *Z. album* crude extract and its isolated compounds, zygo-albuside **A** and rutin, significantly attenuated testicular damage through suppressing apoptosis via inhibition of the p53 pathway and downregulation of miRNA-29a. The investigated *Z. album* extract and its isolated compounds zygo-albuside **A** and rutin also reduced inflammation via downregulation of NF- κ B and reduction of proinflammatory cytokines and enhanced the antioxidant capacity by increasing SOD and CAT. The current study provides a new promising natural product, zygo-albuside **A**, as a potential counteracting agent against MTX side effects on testis. Complete assessment of the toxicity profile of the newly isolated compound zygo-albuside **A** is required in future studies to indicate its therapeutic index.

Supplementary Materials: The supporting information can be downloaded at: <https://www.mdpi.com/article/10.3390/ijms231810799/s1>.

Author Contributions: Conceptualization, J.M.B., S.A.A., A.K.I., M.S.A.-K. and E.T.M.; methodology, R.F.A.A., E.E.E., D.M.H., E.T.M. and S.M.M.; validation, R.F.A.A., E.E.E., D.M.H. and J.M.B.; formal analysis, M.S.A.-K.; investigation, E.T.M., S.M.M., E.E.E. and R.F.A.A. resources, D.M.H.; data curation, E.E.E., R.F.A.A. and S.A.F.; writing—original draft preparation, D.M.H. and S.A.F.; writing—review and editing, E.T.M., E.E.E. and R.F.A.A.; supervision, J.M.B., A.K.I. and S.A.A.; project administration, J.M.B., A.K.I. and S.A.A.; funding acquisition, M.S.A.-K. All authors have read and agreed to the published version of the manuscript.

Funding: This research received no external funding.

Institutional Review Board Statement: The study protocol was approved by the ethical committee of the Faculty of Pharmacy at Suez Canal University (approval number: 202010PHDA1).

Informed Consent Statement: Not applicable.

Data Availability Statement: Not applicable.

Acknowledgments: This publication was supported by the Deanship of Scientific Research at Prince Sattam Bin Abdulaziz University, Al-Kharj, Saudi Arabia, as well as by Suez Canal University, Ismailia, Egypt.

Conflicts of Interest: The authors declare no conflict of interest.

References

1. Khan, Z.A.; Tripathi, R.; Mishra, B. Methotrexate: A detailed review on drug delivery and clinical aspects. *Expert Opin. Drug Deliv.* **2012**, *9*, 151. [[CrossRef](#)] [[PubMed](#)]
2. Armagan, A.; Uzar, E.; Uz, E.; Yilmaz, H.R.; Kutluhan, S.; Koyuncuoglu, H.R.; Soyupek, S.; Cam, H.; Serel, T.A. Caffeic acid phenethyl ester modulates methotrexate-induced oxidative stress in testes of rat. *Hum. Exp. Toxicol.* **2008**, *27*, 547. [[CrossRef](#)] [[PubMed](#)]
3. Owumi, S.E.; Ochaoga, S.E.; Odunola, O.A.; Farombi, E.O. Protocatechuic acid inhibits testicular and epididymal toxicity associated with methotrexate in rats. *Andrologia* **2019**, *51*, e13350. [[CrossRef](#)] [[PubMed](#)]
4. Sheikhabahaei, F.; Khazaei, M.; Rabzia, A.; Mansouri, K.; Ghanbari, A. Protective Effects of Thymoquinone against Methotrexate-Induced Germ Cell Apoptosis in Male Mice. *Int. J. Fertil. Steril.* **2016**, *9*, 541.
5. Vardi, N.; Parlakpınar, H.; Ates, B.; Cetin, A.; Oflu, A. Antiapoptotic and antioxidant effects of beta-carotene against methotrexate-induced testicular injury. *Fertil. Steril.* **2009**, *92*, 2028. [[CrossRef](#)]
6. Wang, Y.; Zhao, T.T.; Zhao, H.Y.; Wang, H. Melatonin protects methotrexate-induced testicular injury in rats. *Eur. Rev. Med. Pharmacol. Sci.* **2018**, *22*, 7517.
7. Belhan, S.; Çomaklı, S.; Küçükler, S.; Gülyüz, F.; Yıldırım, S.; Yener, Z. Effect of chrysin on methotrexate-induced testicular damage in rats. *Andrologia* **2019**, *51*, e13145. [[CrossRef](#)]
8. Dutta, S.; Sengupta, P.; Slama, P.; Roychoudhury, S. Oxidative Stress, Testicular Inflammatory Pathways, and Male Reproduction. *Int. J. Mol. Sci.* **2021**, *22*, 10043. [[CrossRef](#)]
9. Quinn, J.J.; Chang, H.Y. Unique features of long non-coding RNA biogenesis and function. *Nat. Rev. Genet.* **2016**, *17*, 47–62. [[CrossRef](#)]
10. Wu, P.; Wang, Q.; Jiang, C.; Chen, C.; Liu, Y.; Chen, Y.; Zeng, Y. MicroRNA-29a is involved lipid metabolism dysfunction and insulin resistance in C₂C₁₂ myotubes by targeting PPAR δ . *Mol. Med. Rep.* **2018**, *17*, 8493. [[CrossRef](#)]
11. Jafarinejad-Farsangi, S.; Farazmand, A.; Mahmoudi, M.; Gharibdoost, F.; Karimizadeh, E.; Noorbakhsh, F.; Faridani, H.; Jamshidi, A.R. MicroRNA-29a induces apoptosis via increasing the Bax:Bcl-2 ratio in dermal fibroblasts of patients with systemic sclerosis. *Autoimmunity* **2015**, *48*, 369. [[CrossRef](#)] [[PubMed](#)]
12. Ding, S.; Liu, D.; Wang, L.; Wang, G.; Zhu, Y. Inhibiting MicroRNA-29a Protects Myocardial Ischemia-Reperfusion Injury by Targeting SIRT1 and Suppressing Oxidative Stress and NLRP3-Mediated Pyroptosis Pathway. *J. Pharmacol. Exp. Ther.* **2020**, *372*, 128. [[CrossRef](#)] [[PubMed](#)]
13. Sherif, I.O.; Al-Mutabagani, L.A.; Sarhan, O.M. *Ginkgo biloba* Extract Attenuates Methotrexate-Induced Testicular Injury in Rats: Cross-talk Between Oxidative Stress, Inflammation, Apoptosis, and miRNA-29a Expression. *Integr. Cancer Ther.* **2020**, *19*, 1534735420969814. [[CrossRef](#)] [[PubMed](#)]
14. Elhady, S.S.; Abdelhameed, R.F.A.; Mehanna, E.T.; Wahba, A.S.; Elfaky, M.A.; Koshak, A.E.; Noor, A.O.; Bogari, H.A.; Malatani, R.T.; Goda, M.S. Metabolic Profiling, Chemical Composition, Antioxidant Capacity, and In Vivo Hepato- and Nephroprotective Effects of *Sonchus cornutus* in Mice Exposed to Cisplatin. *Antioxidants* **2022**, *11*, 819. [[CrossRef](#)] [[PubMed](#)]
15. Eltamany, E.E.; Elhady, S.S.; Nafie, M.S.; Ahmed, H.A.; Abo-Elmatty, D.M.; Ahmed, S.A.; Badr, J.M.; Abdel-Hamed, A.R. The Antioxidant *Carrichtera annua* DC. Ethanolic Extract Counteracts Cisplatin Triggered Hepatic and Renal Toxicities. *Antioxidants* **2021**, *10*, 825. [[CrossRef](#)]
16. Kim, J.S.; Kim, K.S.; Son, J.Y.; Kim, H.R.; Park, J.H.; Lee, S.H.; Lee, D.E.; Kim, I.S.; Lee, K.Y.; Lee, B.M.; et al. Protective effects of *Dendropanax moribifera* against cisplatin-induced nephrotoxicity without altering chemotherapeutic efficacy. *Antioxidants* **2019**, *8*, 256. [[CrossRef](#)]
17. Soliman, A.M.; Desouky, S.; Marzouk, M.; Sayed, A.A. *Origanum majorana* attenuates nephrotoxicity of cisplatin anticancer drug through ameliorating oxidative stress. *Nutrients* **2016**, *8*, 264. [[CrossRef](#)]
18. Heidari-Soreshjani, S.; Asadi-Samani, M.; Yang, Q.; Saedi-Boroujeni, A. Phytotherapy of nephrotoxicity-induced by cancer drugs: An updated review. *J. Nephropathol.* **2017**, *6*, 254. [[CrossRef](#)]
19. Ilyas, S.; Tabasum, R.; Iftikhar, A.; Nazir, M.; Hussain, A.; Hussain, A.; Ali, M.S.; Saleem, F.; Saleem, U.; Froeyen, M.; et al. Effect of *Berberis vulgaris* L. root extract on ifosfamide-induced in vivo toxicity and in vitro cytotoxicity. *Sci. Rep.* **2021**, *11*, 1708. [[CrossRef](#)]
20. Ilari, S.; Lauro, F.; Giancotti, L.A.; Malafoglia, V.; Dagostino, C.; Gliozzi, M.; Condemi, A.; Maiuolo, J.; Oppedisano, F.; Palma, E.; et al. The Protective Effect of Bergamot Polyphenolic Fraction (BPF) on Chemotherapy-Induced Neuropathic Pain. *Pharmaceuticals* **2021**, *14*, 975. [[CrossRef](#)]
21. Hannan, M.A.; Zahan, M.S.; Sarker, P.P.; Moni, A.; Ha, H.; Uddin, M.J. Protective Effects of Black Cumin (*Nigella sativa*) and Its Bioactive Constituent, Thymoquinone against Kidney Injury: An Aspect on Pharmacological Insights. *Int. J. Mol. Sci.* **2021**, *22*, 9078. [[CrossRef](#)] [[PubMed](#)]
22. Jiang, Y.; Zhang, Z.; Cha, L.; Li, L.; Zhu, D.; Fang, Z.; He, Z.; Huang, J.; Pan, Z. Resveratrol Plays a Protective Role against Premature Ovarian Failure and Prompts Female Germline Stem Cell Survival. *Int. J. Mol. Sci.* **2019**, *20*, 3605. [[CrossRef](#)] [[PubMed](#)]
23. Miyata, Y.; Sakai, H. Anti-Cancer and Protective Effects of Royal Jelly for Therapy-Induced Toxicities in Malignancies. *Int. J. Mol. Sci.* **2018**, *19*, 3270. [[CrossRef](#)]
24. Martins, R.V.L.; Silva, A.M.S.; Duarte, A.P.; Socorro, S.; Correia, S.; Maia, C.J. Natural Products as Protective Agents for Male Fertility. *BioChem* **2021**, *1*, 122–147. [[CrossRef](#)]

25. Timar, M.; Banaei, S.; Mehraban, Z.; Salimnejad, R.; Golmohammadi, M.G. Protective effect of saponin on sperm DNA fragmentation of mice treated with cyclophosphamide. *Andrologia* **2022**, *54*, e14336. [[CrossRef](#)] [[PubMed](#)]
26. Noh, S.; Go, A.; Kim, D.B.; Park, M.; Jeon, H.W.; Kim, B. Role of Antioxidant Natural Products in Management of Infertility: A Review of Their Medicinal Potential. *Antioxidants* **2020**, *9*, 957. [[CrossRef](#)]
27. Ștefănescu, R.; Farczadi, L.; Huțanu, A.; Ósz, B.E.; Mărușteri, M.; Negroiu, A.; Vari, C.E. Tribulus terrestris Efficacy and Safety Concerns in Diabetes and Erectile Dysfunction, Assessed in an Experimental Model. *Plants* **2021**, *10*, 744. [[CrossRef](#)]
28. Fernández-Lázaro, D.; Mielgo-Ayuso, J.; del Valle Soto, M.; Adams, D.P.; González-Bernal, J.J.; Seco-Calvo, J. The Effects of 6 Weeks of *Tribulus terrestris* L. Supplementation on Body Composition, Hormonal Response, Perceived Exertion, and CrossFit®Performance: A Randomized, Single-Blind, Placebo-Controlled Study. *Nutrients* **2021**, *13*, 3969. [[CrossRef](#)]
29. Shehzad, M.; Rasheed, H.; Naqvi, S.A.; Al-Khayri, J.M.; Lorenzo, J.M.; Alaghbari, M.A.; Manzoor, M.F.; Aadil, R.M. Therapeutic Potential of Date Palm against Human Infertility: A Review. *Metabolites* **2021**, *11*, 408. [[CrossRef](#)]
30. Tauchen, J.; Jurášek, M.; Huml, L.; Rimpelová, S. Medicinal Use of Testosterone and Related Steroids Revisited. *Molecules* **2021**, *26*, 1032. [[CrossRef](#)]
31. Mesbahzadeh, B.; Hassanzadeh-Taheri, M.; Baniasadi, P.; Hosseini, M. The protective effect of crocin on cisplatin-induced testicular impairment in rats. *BMC Urol.* **2021**, *21*, 117. [[CrossRef](#)] [[PubMed](#)]
32. Sönmez, M.F.; Çilenk, K.T.; Karabulut, D.; Ünalmiş, S.; Deligönül, E.; Öztürk, İ.; Kaymak, E. Protective effects of propolis on methotrexate-induced testis injury in rat. *Biomed. Pharmacother.* **2016**, *79*, 44. [[CrossRef](#)] [[PubMed](#)]
33. Morsy, M.A.; Abdel-Aziz, A.M.; Abdel-Hafez, S.M.N.; Venugopala, K.N.; Nair, A.B.; Abdel-Gaber, S.A. The Possible Contribution of P-Glycoprotein in the Protective Effect of Paeonol against Methotrexate-Induced Testicular Injury in Rats. *Pharmaceuticals* **2020**, *13*, 223. [[CrossRef](#)] [[PubMed](#)]
34. Ajayi, L.; Ayeleso, A.; Oyedepo, T.; Mukwevho, E. Ameliorative Potential of Hydroethanolic Leaf Extract of *Parquetina nigrescens* on d-Galactose-Induced Testicular Injury. *Molecules* **2021**, *26*, 3424. [[CrossRef](#)]
35. Zhang, Q.; Yang, C.; Zhang, M.; Lu, X.; Cao, W.; Xie, C.; Li, X.; Wu, J.; Zhong, C.; Geng, S. Protective effects of ginseng stem-leaf saponins on D-galactose-induced reproductive injury in male mice. *Aging* **2021**, *13*, 8916. [[CrossRef](#)]
36. Leng, J.; Hou, J.; Fu, C.; Ren, S.; Jiang, S.; Wang, Y.; Chen, C.; Wang, Z. *Platycodon grandiflorum* Saponins attenuate scrotal heat-induced spermatogenic damage via inhibition of oxidative stress and apoptosis in mice. *J. Funct. Foods* **2019**, *54*, 479. [[CrossRef](#)]
37. Liu, W.; Leng, J.; Hou, J.G.; Jiang, S.; Wang, Z.; Liu, Z.; Gong, X.J.; Chen, C.; Wang, Y.P.; Li, W. Saponins derived from the stems and leaves of *Panax ginseng* attenuate scrotal heat-induced spermatogenic damage via inhibiting the MAPK mediated oxidative stress and apoptosis in mice. *Phytother. Res.* **2021**, *35*, 311. [[CrossRef](#)]
38. Vyas, R.; Kesari, K.K.; Slama, P.; Roychoudhury, S.; Sisodia, R. Differential Activity of Antioxidants in Testicular Tissues Following Administration of Chlorophytum borivilianum in Gamma-Irradiated Swiss Albino Mice. *Front. Pharmacol.* **2022**, *17*, 12. [[CrossRef](#)]
39. Leung, K.W.; Wong, A.S. Ginseng and male reproductive function. *Spermatogenesis* **2013**, *3*, e26391. [[CrossRef](#)]
40. Obidiegwu, J.E.; Lyons, J.B.; Chilaka, C.A. The *Dioscorea* Genus (Yam)—An Appraisal of Nutritional and Therapeutic Potentials. *Foods* **2020**, *9*, 1304. [[CrossRef](#)]
41. Hussein, S.R.; Kawashty, S.A.; Tantawy, M.E.; Saleh, A.M. Nabel. Chemosystematic studies of *Nitraria retusa* and selected taxa of Zygophyllaceae in Egypt. *Plant Syst. Evol.* **2009**, *277*, 251. [[CrossRef](#)]
42. Sheahan, D.F.; Cutler, F.L.S. Contribution of vegetative anatomy to the systematics of the Zygophyllaceae. *Bot. J. Linn. Soc.* **1993**, *113*, 227. [[CrossRef](#)]
43. Shawky, E.; Gabr, N.; El-gindi, M.; Mekky, R. A comprehensive review on genus *Zygophyllum*. *J. Adv. Pharm. Res.* **2019**, *3*, 1. [[CrossRef](#)]
44. Nabel, A.M.; Saleh, M.N. An approach to the chemosystematics of the Zygophyllaceae. *Biochem. Syst. Ecol.* **1977**, *5*, 121–128.
45. Aboul-Enein, A.M.; El-Ela, F.A.; Shalaby, E.A.; El-Shemy, H.A. Traditional medicinal plants research in Egypt: Studies of antioxidant and anticancer activities. *J. Med. Plant Res.* **2012**, *6*, 689.
46. Kchaou, M.; Ben-Salah, H.; Mnafigui, K.; Abdennabi, R.; Gharsallah, N.; Elfeki, A.; Damak, M.; Allouche, N. Chemical composition and biological activities of *Zygophyllum album* (L.) essential oil from Tunisia. *J. Agric. Sci. Technol.* **2016**, *18*, 1499.
47. Bourgou, S.; Megdiche, W.; Ksouri, R. The halophytic genus *Zygophyllum* and *Nitraria* from North Africa: A phytochemical and pharmacological overview. *Med. Aromat. Plants* **2017**, *3*, 345.
48. Ouffai, K.; Rachid, A.Z.Z.I.; Abboou, F.; Lahfa, F.B. Antihemolytic and antioxidant activities of aerial parts extracts of *Zygophyllum album* L. and *Globularia alypum* L. from Algeria. *JNPRA* **2022**, *1*, 41. [[CrossRef](#)]
49. Mnafigui, K.; Kchaou, M.; Hamden, K.; Derbali, F.; Slama, S.; Nasri, M.; Salah, H.B.; Allouche, N.; Elfeki, A. Inhibition of carbohydrate and lipid digestive enzymes activities by *Zygophyllum album* extracts: Effect on blood and pancreas inflammatory biomarkers in alloxan-induced diabetic rats. *J. Physiol. Biochem.* **2014**, *70*, 93. [[CrossRef](#)]
50. Mnafigui, K.; Kchaou, M.; Ben-Salah, H.; Hajji, R.; Khabbabi, G.; Elfeki, A.; Allouche, N.; Gharsallah, N. Essential oil of *Zygophyllum album* inhibits key-digestive enzymes related to diabetes and hypertension and attenuates symptoms of diarrhea in alloxan-induced diabetic rats. *Pharm. Biol.* **2016**, *54*, 1326. [[CrossRef](#)]
51. Ghouli, J.E.; Boughattas, N.A.; Ben Attia, M. Antihyperglycemic and antihyperlipidemic activities of ethanolic extract of *Zygophyllum album* in streptozotocin-induced diabetic mice. *Toxicol. Ind. Health* **2013**, *29*, 43. [[CrossRef](#)] [[PubMed](#)]

52. Mnafigui, K.; Hamden, K.; Ben Salah, H.; Kchaou, M.; Nasri, M.; Slama, S.; Derbali, F.; Allouche, N.; Elfeki, A. Inhibitory Activities of *Zygophyllum album*: A Natural Weight-Lowering Plant on Key Enzymes in High-Fat Diet-Fed Rats. *Evid.-Based Complement. Altern. Med.* **2012**, *2012*, 620384. [[CrossRef](#)] [[PubMed](#)]
53. Feriani, A.; Tir, M.; Gómez-Caravaca, A.M.; Del Mar Contreras, M.; Talhaoui, N.; Taamalli, A.; Segura-Carretero, A.; Ghazouani, L.; Mufti, A.; Tlili, N.; et al. HPLC-DAD-ESI-QTOF- MS/MS profiling of *Zygophyllum album* roots extract and assessment of its cardioprotective effect against deltamethrin-induced myocardial injuries in rat, by suppression of oxidative stress-related inflammation and apoptosis via NF- κ B signaling pathway. *J. Ethnopharmacol.* **2020**, *247*, 112266. [[PubMed](#)]
54. Tigrine-Kordjani, N.; Meklati, B.Y.; Chemat, F. Contribution of microwave accelerated distillation in the extraction of the essential oil of *Zygophyllum album* L. *Phytochem. Anal.* **2010**, *22*, 1–9. [[CrossRef](#)] [[PubMed](#)]
55. Hasanean, H.A.; El-Shanawany, M.A.; Bishay, D.W.; Franz, G. Saponins from *Zygophyllum album* L. *Bull. Pharm. Sci. Assiut* **1989**, *12*, 117. [[CrossRef](#)]
56. Hasanean, H.H.; Desoky, E.K.; El-Hamouly, M.M.A. Quinovic acid glycosides from *Zygophyllum album*. *Phytochemistry* **1993**, *33*, 663. [[CrossRef](#)]
57. Hasanean, H.; El-Hamouly, M.; El-Moghazy, S.; Bishay, D. 14-decarboxyquinovic and quinovic acid glycosides from *Zygophyllum album*. *Phytochemistry* **1993**, *33*, 667. [[CrossRef](#)]
58. Elgamal, M.H.A.; Shaker, K.H.; Pöllmann, K.; Seifert, K. Triterpenoid saponins from *Zygophyllum* species. *Phytochemistry* **1995**, *40*, 1233. [[CrossRef](#)]
59. Hussein, S.; Marzouk, M.; Ibrahim, L.; Kawashty, S.; Saleh, N. Flavonoids of *Zygophyllum album* L. and *Zygophyllum simplex* L. (Zygophyllaceae). *Biochem. Syst. Ecol.* **2011**, *39*, 778. [[CrossRef](#)]
60. Chaturvedula, V.S.P.; Prakash, I. Isolation of Stigmasterol and β -Sitosterol from the dichloromethane extract of *Rubus suavisissimus*. *Int. Curr. Pharm. J.* **2012**, *1*, 239. [[CrossRef](#)]
61. Seebacher, W.; Simic, N.; Weis, R.; Saf, R.; Kunert, O. Complete assignments of ^1H and ^{13}C NMR resonances of oleanolic acid, 18α -oleanolic acid, ursolic acid and their 11-oxo derivatives. *Magn. Reson. Chem.* **2003**, *41*, 636. [[CrossRef](#)]
62. Tshilanda, D.D.; Onyamboko, D.N.; Babady-Bila, P.; Ngbolua, K.T.N.; Tshibangu, D.S.; Mpiana, P.T. Anti-sickling activity of ursolic acid isolated from the leaves of *Ocimum gratissimum* L. (Lamiaceae). *Nat. Prod. Bioprospect.* **2015**, *5*, 215. [[CrossRef](#)] [[PubMed](#)]
63. Abd ELnasser, B.S.; El Dina, M.Y.; Elgindi, M.R.; Elsaid, M.B. Biological studies of isolated triterpenoids and phenolic compounds identified from *Wodyetia bifurcata* family Arecaceae. *J. Pharmacogn. Phytochem.* **2015**, *3*, 67.
64. Chang, S.W.; Kim, K.H.; Lee, I.K.; Choi, S.U.; Ryu, S.Y.; Lee, K.R. Phytochemical constituents of *Bistorta manshuriensis*. *Nat. Prod. Sci.* **2009**, *15*, 234.
65. Kim, J.W.; Kim, T.B.; Yang, H.; Sung, S.H. Phenolic compounds isolated from *Opuntia ficus-indica* fruits. *Nat. Prod. Sci.* **2016**, *22*, 117. [[CrossRef](#)]
66. Renda, G.; Ozgen, U.; Unal, Z.; Sabuncuoglu, S.; Palaska, E.; Orhan, I.E. Flavonoid derivatives from the aerial parts of *Trifolium trichocephalum* M. Bieb. and their antioxidant and cytotoxic activity. *Rec. Nat. Prod.* **2017**, *11*, 479. [[CrossRef](#)]
67. Gupta, J.; Gupta, A. Isolation and identification of flavonoid rutin from *Rauwolfia serpentina*. *Int. J. Chem. Stud.* **2015**, *3*, 113.
68. Kitajima, J.; Shindo, M.; Tanaka, Y. Two new triterpenoid sulfates from the leaves of *Schefflera octophylla*. *Chem. Pharm. Bull.* **1990**, *38*, 714. [[CrossRef](#)]
69. Figueroa, F.A.; Abdala-Díaz, R.T.; Pérez, C.; Casas-Arrojo, V.; Nesic, A.; Tapia, C.; Durán, C.; Valdes, O.; Parra, C.; Bravo-Arrepol, G.; et al. Sulfated Polysaccharide Extracted from the Green Algae *Codium bernabei*: Physicochemical Characterization and Antioxidant, Anticoagulant and Antitumor Activity. *Mar. Drugs* **2022**, *20*, 458. [[CrossRef](#)]
70. Kellner Filho, L.C.; Picão, B.W.; Silva, M.L.A.; Cunha, W.R.; Pauletti, P.M.; Dias, G.M.; Copp, B.R.; Bertanha, C.S.; Janeiro, A.H. Bioactive Aliphatic Sulfates from Marine Invertebrates. *Mar. Drugs* **2019**, *17*, 527. [[CrossRef](#)]
71. Chen, S.-K.; Hsu, C.-H.; Tsai, M.-L.; Chen, R.-H.; Drummen, G.P.C. Inhibition of Oxidative Stress by Low-Molecular-Weight Polysaccharides with Various Functional Groups in Skin Fibroblasts. *Int. J. Mol. Sci.* **2013**, *14*, 19399. [[CrossRef](#)] [[PubMed](#)]
72. Safir, O.; Fkih-Tetouani, S.; De Tommasi, N.; Aquino, R. Saponins from *Zygophyllum gaetulum*. *J. Nat. Prod.* **1998**, *61*, 130. [[CrossRef](#)] [[PubMed](#)]
73. Olszewska, M. Flavonoids from *Prunus serotina* ehrh. *Acta Pol. Pharm.* **2005**, *62*, 127. [[PubMed](#)]
74. Silverstein, R.M.; Webster, F.X.; Kiemle, D.J. *Spectrometric Identification of Organic Compounds*, 3rd ed.; John Wiley & Sons: New York, NY, USA, 1974.
75. Natori, T.; Morita, M.; Akimoto, K.; Koezuka, Y. Agelasphins, novel antitumor and immunostimulatory cerebroside from the marine sponge *Agelas mauritanus*. *Tetrahedron. Lett.* **1994**, *50*, 2771. [[CrossRef](#)]
76. Thomford, A.K.; Abdelhameed, R.F.A.; Yamada, K. Chemical studies on the parasitic plant *Thonningia sanguinea* Vahl. *RSC Adv.* **2018**, *8*, 21002. [[CrossRef](#)]
77. Feng, Y.L.; Wu, B.; Li, H.R.; Li, Y.Q.; Xu, L.Z.; Yang, S.L.; Kitanaka, S. Triterpenoidal saponins from the barks of *Zygophyllum fabago* L. *Chem. Pharm. Bull.* **2008**, *56*, 858. [[CrossRef](#)]
78. Popova, O.I.; Murav'eva, D.A. Ursolic acid from leafy shoots of *Viscum album*. *Chem. Nat. Compd.* **1990**, *26*, 346. [[CrossRef](#)]
79. Lim Ah Tock, M.; Combrinck, S.; Kamatou, G.; Chen, W.; Van Vuuren, S.; Viljoen, A. Antibacterial Screening, Biochemometric and Bioautographic Evaluation of the Non-Volatile Bioactive Components of Three Indigenous South African *Salvia* Species. *Antibiotics* **2022**, *11*, 901. [[CrossRef](#)]

80. Parvez, M.K.; Alam, P.; Arbab, A.H.; Al-Dosari, M.S.; Alhowiriny, T.A.; Alqasoumi, S.I. Analysis of antioxidative and antiviral biomarkers β -amyrin, β -sitosterol, lupeol, ursolic acid in *Guiera senegalensis* leaves extract by validated HPTLC methods. *Saudi Pharm. J.* **2018**, *26*, 685. [[CrossRef](#)]
81. Adachi, S. Thin-Layer Chromatography of carbohydrates in the presence of bisulfite. *J. Chromatogr.* **1965**, *17*, 295. [[CrossRef](#)]
82. Harborne, J.B. Sugars and their Derivatives. In *Phytochemical Methods*, 2nd ed.; Chapman and Hall: London, UK, 1984; pp. 222–242.
83. Amin, E.; El-Hawary, S.S.; Fathy, M.M.; Mohammed, R.; Ali, Z.; Khan, I.A. Zygophylloside S, a New Triterpenoid Saponin from the Aerial Parts of *Zygophyllum coccineum* L. *Planta Med.* **2010**, *76*, 51. [[CrossRef](#)]
84. Eltamany, E.E.; Elhady, S.S.; Ahmed, H.A.; Badr, J.M.; Noor, A.O.; Ahmed, S.A.; Nafie, M.S. Chemical Profiling, Antioxidant, Cytotoxic Activities and Molecular Docking Simulation of *Carrichtera Annuia* DC. (Cruciferae). *Antioxidants* **2020**, *9*, 1286. [[CrossRef](#)] [[PubMed](#)]
85. Grassmann, J. Terpenoids as Plant Antioxidants. *Vitam. Horm.* **2005**, *72*, 505. [[PubMed](#)]
86. Belguidoum, M.; Dendougui, H.; Kendour, Z. In vitro antioxidant properties and phenolic contents of *Zygophyllum album* L. from Algeria. *J. Chem. Pharm. Res.* **2015**, *2015*, 510.
87. Mostafa, R.; Essawy, H. Ecophysiological analysis of *Zygophyllum album* plant and its allelopathy. In Proceedings of the 6th International Conference, Menoufia University, Al Minufiyah, Egypt, 11–12 May 2016.
88. Lfitat, A.; Zejli, H.; Bousraf, F.; Bousselham, A.; El Atki, Y.; Gouch, A.; Badiia, L.; Abdellaoui, A. Comparative Assessment of Total Phenolics Content and in vitro Antioxidant Capacity Variations of Macerated Leaf Extracts of *Olea europaea* L. and *Argania Spinosa* (L.) Skeels. *Mater. Today Proc.* **2021**, *45*, 7271. [[CrossRef](#)]
89. Aryal, S.; Baniya, M.K.; Danekhu, K.; Kunwar, P.; Gurung, R.; Koirala, N. Total Phenolic Content, Flavonoid Content and Antioxidant Potential of Wild Vegetables from Western Nepal. *Plants* **2019**, *8*, 96. [[CrossRef](#)]
90. Buettner, G.R. Superoxide dismutase in redox biology: The roles of superoxide and hydrogen peroxide. *Anti-Cancer Agents Med. Chem.* **2011**, *11*, 341. [[CrossRef](#)]
91. Mahmoud, E.A.; Sankaranarayanan, J.; Morachis, J.M.; Kim, G.; Almutairi, A. Inflammation responsive logic gate nanoparticles for the delivery of proteins. *Bioconjug. Chem.* **2011**, *22*, 1416. [[CrossRef](#)]
92. De Gracia Lux, C.; Joshi-Barr, S.; Nguyen, T.; Mahmoud, E.; Schopf, E.; Fomina, N.; Almutairi, A. Biocompatible polymeric nanoparticles degrade and release cargo in response to biologically relevant levels of hydrogen peroxide. *J. Am. Chem. Soc.* **2012**, *134*, 15758. [[CrossRef](#)]
93. Saed-Moucheshi, A.; Pakniyat, H.; Pirasteh-Anosheh, H.; Azoos, M.M. Chapter 20—Role of ROS as Signaling Molecules in Plants. In *Oxidative Damage to Plants*; Ahmad, P., Ed.; Academic Press: San Diego, CA, USA, 2014; p. 585.
94. Shen, Y.; White, E. p53-dependent apoptosis pathways. *Adv. Cancer Res.* **2001**, *82*, 8255.
95. Akhtar, R.S.; Ness, J.M.; Roth, K.A. Bcl-2 family regulation of neuronal development and neurodegeneration. *Biochim. Biophys. Acta* **2004**, *1644*, 189. [[CrossRef](#)]
96. Pınar, N.; Çakırca, G.; Özgür, T.; Kaplan, M. The protective effects of alpha lipoic acid on methotrexate induced testis injury in rats. *Biomed. Pharmacother.* **2018**, *97*, 1486. [[CrossRef](#)] [[PubMed](#)]
97. Ibrahim, M.A.; El-Sheikh, A.A.K.; Khalaf, H.M.; Abdelrahman, A.M. Protective effect of peroxisome proliferator activator receptor (PPAR)- α and - γ ligands against methotrexate-induced nephrotoxicity. *Immunopharmacol. Immunotoxicol.* **2014**, *36*, 130. [[CrossRef](#)] [[PubMed](#)]
98. Asadi, N.; Bahmani, M.; Kheradmand, A.; Rafieian-Kopaei, M. The Impact of Oxidative Stress on Testicular Function and the Role of Antioxidants in Improving it: A Review. *J. Clin. Diagn. Res.* **2017**, *11*, 1e01. [[CrossRef](#)] [[PubMed](#)]
99. Sikka, S.C. Relative impact of oxidative stress on male reproductive function. *Curr. Med. Chem.* **2001**, *8*, 851. [[CrossRef](#)] [[PubMed](#)]
100. Moustafa, M.H.; Sharma, R.K.; Thornton, J.; Mascha, E.; Abdel-Hafez, M.A.; Thomas, A.J.; Agarwal, A. Relationship between ROS production, apoptosis and DNA denaturation in spermatozoa from patients examined for infertility. *Hum. Reprod.* **2004**, *19*, 129. [[CrossRef](#)]
101. Lysiak, J.J. The role of tumor necrosis factor-alpha and interleukin-1 in the mammalian testis and their involvement in testicular torsion and autoimmune orchitis. *Reprod. Biol. Endocrinol.* **2004**, *2*, 9. [[CrossRef](#)]
102. Makary, S.; Abdo, M.; Fekry, E. Oxidative stress burden inhibits spermatogenesis in adult male rats: Testosterone protective effect. *Can. J. Physiol. Pharmacol.* **2018**, *96*, 372. [[CrossRef](#)]
103. Lysiak, J.J.; Nguyen, Q.A.; Kirby, J.L.; Turner, T.T. Ischemia-reperfusion of the murine testis stimulates the expression of proinflammatory cytokines and activation of c-jun N-terminal kinase in a pathway to E-selectin expression. *Biol. Reprod.* **2003**, *69*, 202. [[CrossRef](#)]
104. Hayden, M.S.; Ghosh, S. Regulation of NF- κ B by TNF family cytokines. *Semin. Immunol.* **2014**, *26*, 253. [[CrossRef](#)]
105. Siddiqui, W.A.; Ahad, A.; Ahsan, H. The mystery of BCL2 family: Bcl-2 proteins and apoptosis: An update. *Arch. Toxicol.* **2015**, *89*, 289. [[CrossRef](#)] [[PubMed](#)]
106. Ezeh, U.I.; Moore, H.D.; Cooke, I.D. Correlation of testicular sperm extraction with morphological, biophysical and endocrine profiles in men with azoospermia due to primary gonadal failure. *Hum. Reprod.* **1998**, *13*, 3066. [[CrossRef](#)] [[PubMed](#)]
107. Meunier, L.; Siddeek, B.; Vega, A.; Lakhdari, N.; Inoubli, L.; Bellon, R.P.; Lemaire, G.; Mauduit, C.; Benahmed, M. Perinatal programming of adult rat germ cell death after exposure to xenoestrogens: Role of microRNA miR-29 family in the downregulation of DNA methyltransferases and Mcl-1. *Endocrinology* **2012**, *153*, 1936. [[CrossRef](#)]

108. Park, S.Y.; Lee, J.H.; Ha, M.; Nam, J.W.; Kim, V.N. miR-29 miRNAs activate p53 by targeting p85 alpha and CDC42. *Nat. Struct. Mol. Biol.* **2009**, *16*, 23. [[CrossRef](#)] [[PubMed](#)]
109. Tang, B.; Li, X.; Ren, Y.; Wang, J.; Xu, D.; Hang, Y.; Zhou, T.; Li, F.; Wang, L. MicroRNA-29a regulates lipopolysaccharide (LPS)-induced inflammatory responses in murine macrophages through the Akt1/ NF- κ B pathway. *Exp. Cell Res.* **2017**, *360*, 74. [[CrossRef](#)] [[PubMed](#)]
110. González-Madariaga, Y.; Mena-Linares, Y.; Martín-Montegudo, D.; Valido-Díaz, A.; Guerra-de-León, J.; Nieto-Reyes, L. In vivo anti-inflammatory effect of saponin-enriched fraction from *Agave brittoniana* Trel subspecies *brachypus*. *Ars Pharm.* **2020**, *61*, 231.
111. Grabowska, K.; Wróbel, D.; Żmudzki, P.; Podolak, I. Anti-inflammatory activity of saponins from roots of *Impatiens parviflora* DC. *Nat. Prod. Res.* **2020**, *34*, 1581. [[CrossRef](#)]
112. Su, S.; Li, X.; Li, S.; Ming, P.; Huang, Y.; Dong, Y.; Ding, H.; Feng, S.; Li, J.; Wang, X.; et al. Rutin protects against lipopolysaccharide-induced mastitis by inhibiting the activation of the NF- κ B signaling pathway and attenuating endoplasmic reticulum stress. *Inflammopharmacology* **2019**, *27*, 77. [[CrossRef](#)]
113. Ma, B.; Meng, X.; Wang, J.; Sun, J.; Ren, X.; Qin, M.; Sun, J.; Sun, G.; Sun, X. Notoginsenoside R1 attenuates amyloid- β -induced damage in neurons by inhibiting reactive oxygen species and modulating MAPK activation. *Int. Immunopharmacol.* **2014**, *22*, 151. [[CrossRef](#)]
114. Sen, S.; Makkar, H.P.; Becker, K. Alfalfa Saponins and Their Implication in Animal Nutrition. *J. Agric. Food Chem.* **1998**, *46*, 131. [[CrossRef](#)] [[PubMed](#)]
115. Akondi, B.R.; Challa, S.R.; Akula, A. Protective effects of rutin and naringin in testicular ischemia-reperfusion induced oxidative stress in rats. *J. Reprod. Infertil.* **2011**, *12*, 209. [[PubMed](#)]
116. Alsharif, N.Z.; Hassoun, E.; Bagchi, M.; Lawson, T.; Stohs, S.J. The Effects of Anti-TNF-Alpha Antibody and Dexamethasone on TCDD-Induced Oxidative Stress in Mice. *Pharmacology* **1994**, *48*, 127. [[CrossRef](#)]
117. Chen, F.; Chen, Y.; Kang, X.; Zhou, Z.; Zhang, Z.; Liu, D. Anti-apoptotic function and mechanism of ginseng saponins in Rattus pancreatic β -cells. *Biol. Pharm. Bull.* **2012**, *35*, 1568. [[CrossRef](#)] [[PubMed](#)]
118. Mohamad, H.E.; Abo-elmatty, D.M.; Wahba, N.S.; Shaheen, M.A.; Sakr, R.T.; Wahba, A.S. Influximab and/or MESNA alleviate doxorubicin-induced Alzheimer's disease-like pathology in rats: A new insight into TNF- α /Wnt/ β -catenin signaling pathway. *Life Sci.* **2022**, *301*, 120613. [[CrossRef](#)] [[PubMed](#)]
119. Pollutri, D.; Gramantieri, L.; Bolondi, L.; Fornari, F. TP53/MicroRNA Interplay in Hepatocellular Carcinoma. *Int. J. Mol. Sci.* **2016**, *17*, 2029. [[CrossRef](#)] [[PubMed](#)]
120. Biersack, B. Current state of phenolic and terpenoidal dietary factors and natural products as non-coding RNA/microRNA modulators for improved cancer therapy and prevention. *Non-Coding RNA Res.* **2016**, *1*, 12. [[CrossRef](#)]
121. Lin, Q.; Ma, L.; Liu, Z.; Yang, Z.; Wang, J.; Liu, J.; Jiang, G. Targeting microRNAs: A new action mechanism of natural compounds. *Oncotarget* **2017**, *8*, 15961. [[CrossRef](#)]
122. Lv, B.; Liu, Z.; Wang, S.; Liu, F.; Yang, X.; Hou, J.; Hou, Z.; Chen, B. MiR-29a promotes intestinal epithelial apoptosis in ulcerative colitis by down-regulating Mcl-1. *Int. J. Clin. Exp. Pathol.* **2014**, *7*, 8542.
123. Hu, Y.; Xie, L.; Yu, J.; Fu, H.; Zhou, D.; Liu, H. Inhibition of microRNA-29a alleviates hyperoxia-induced bronchopulmonary dysplasia in neonatal mice via upregulation of GAB1. *Mol. Med.* **2019**, *26*, 3. [[CrossRef](#)]
124. Noman, O.M.; Nasr, F.A.; Mothana, R.A.; Alqahtani, A.S.; Qamar, W.; Al-Mishari, A.A.; Al-Rehaily, A.J.; Siddiqui, N.A.; Alam, P.; Almarfadi, O.M. Isolation, Characterization, and HPTLC-Quantification of Compounds with Anticancer Potential from *Loranthus Acaciae* Zucc. *Separations* **2020**, *7*, 43. [[CrossRef](#)]
125. Gogoi, J.; Nakhuru, K.S.; Policegoudra, R.S.; Chattopadhyay, P.; Rai, A.K.; Veer, V. Isolation, and characterization of bioactive components from *Mirabilis jalapa* L. radix. *J. Tradit. Complement. Med.* **2015**, *6*, 41. [[CrossRef](#)] [[PubMed](#)]
126. Siddiqui, N.A.; Al-Yousef, H.M.; Alhowiriny, T.A.; Alam, P.; Hassan, W.H.B.; Amina, M.; Hussain, A.; Abdelaziz, S.; Abdallah, R.H. Con-current analysis of bioactive triterpenes oleanolic acid and β -amyrin in antioxidant active fractions of *Hibiscus calyphyllus*, *Hibiscus deflersii* and *Hibiscus micranthus* grown in Saudi Arabia by applying validated HPTLC method. *Saudi Pharm. J.* **2018**, *26*, 266. [[CrossRef](#)] [[PubMed](#)]
127. Alam, P.; Alajmi, M.F.; Siddiqui, N.A.; Al-Rehaily, A.J.; Alharbi, H.; Basudan, O.A.; Hussain, A. Densitometric validation and analysis of biomarker β -amyrin in different *Acacia* species (leaves) grown in Kingdom of Saudi Arabia by high performance thin-layer chromatography. *Pak. J. Pharm. Sci.* **2015**, *28*, 1485. [[PubMed](#)]
128. Nile, S.H.; Park, S.W. HPTLC densitometry method for simultaneous determination of flavonoids in selected medicinal plants. *Front. Life Sci.* **2015**, *8*, 103. [[CrossRef](#)]
129. Altemimi, A.B.; Mohammed, M.J.; Yi-Chen, L.; Watson, D.G.; Lakhssassi, N.; Cacciola, F.; Ibrahim, S.A. Optimization of Ultrasonicated Kaempferol Extraction from *Ocimum basilicum* Using a Box-Behnken Design and Its Densitometric Validation. *Foods* **2020**, *9*, 1379. [[CrossRef](#)]
130. Avertseva, I.N.; Suleymanova, F.S.; Nesterova, O.V.; Reshetnyak, V.Y.; Matveenko, V.N.; Zhukov, P.A. Study of Polyphenolic Compounds in Extracts from Flowers and Leaves of Canadian Goldenrod and Dwarf Goldenrod (*Solidago canadensis* L. and *Solidago nana* Nitt.). *Mosc. Univ. Chem. Bull.* **2020**, *75*, 47–51. [[CrossRef](#)]
131. Główniak, K.; Skalicka, K.; Ludwiczuk, A.; Jop, K. Phenolic Compounds in the Flowers of *Lavatera trimestris* L. (Malvaceae). *J. Planar Chromat.* **2005**, *18*, 264–268. [[CrossRef](#)]

132. Wagner, H.; Bladt, S. *Plant Drug Analysis: A Thin Layer Chromatography Atlas*, 2nd ed.; Springer: Heidelberg, Germany, 2009; pp. 195–245.
133. Yen, G.C.; Duh, P.D. Scavenging effect of methanolic extracts of peanut hulls on free-radical and active-oxygen species. *J. Agric. Food Chem.* **1994**, *42*, 629. [[CrossRef](#)]
134. Elaasser, M.M.; Morsi, M.K.; Galal, S.M.; Abd El-Rahman, M.K.; Katry, M.A. Antioxidant, anti-inflammatory and cytotoxic activities of the unsaponifiable fraction of extra virgin olive oil. *Grasas Aceites* **2020**, *71*, e386. [[CrossRef](#)]
135. Ruch, R.J.; Cheng, S.T.; Klauring, J.E. Prevention of cytotoxicity and inhibition of intercellular communication by antioxidant catechins isolated from chinese green tea. *Carcinogenesis* **1989**, *10*, 1003. [[CrossRef](#)]
136. Prieto, P.; Pineda, M.; Aguilar, M. Spectrophotometric quantitation of antioxidant capacity through the formation of a phosphomolybdenum complex: Specific application to the determination of vitamin E. *Anal. Biochem.* **1999**, *269*, 337. [[CrossRef](#)] [[PubMed](#)]
137. Najafi, G.; Atashfaraz, E.; Farokhi, F. Attenuation of Methotrexate-Induced Embryotoxicity and Oxidative Stress by Ethyl Pyruvate. *Int. J. Fertil. Steril.* **2016**, *10*, 232.
138. Ghoul, J.E.; Smiri, M.; Saad, G.; Boughattas, N.A.; Ben-Attia, M. Antihyperglycemic, antihyperlipidemic and antioxidant activities of traditional aqueous extract of *Zygophyllum album* in streptozotocin diabetic mice. *Pathophysiology* **2011**, *19*, 35–42. [[CrossRef](#)] [[PubMed](#)]
139. Liang, Y.; Yang, X.; Zhang, X.; Duan, H.; Jin, M.; Sun, Y.; Yuan, H.; Li, J.; Qi, Y.; Qiao, W. Antidepressant-like effect of the saponins part of ethanol extract from SHF. *J. Ethnopharmacol.* **2016**, *191*, 307–314. [[CrossRef](#)]
140. Patil, S.L.; Somashekarappa, H.; Rajashekhar, K. Radiomodulatory role of Rutin and Quercetin in Swiss Albino mice exposed to the whole body gamma radiation. *Indian J. Nucl. Med.* **2012**, *27*, 237–242. [[CrossRef](#)]